Army Research Laboratory

The Battlescale Forecast Model (BFM) during the TFXXI at Fort Irwin, CA: Statistical Evaluation of 24 h Forecast Fields and Model Improvement

By Teizi Henmi and Robert E. Dumais, Jr.
Information Science & Technology Directorate
Battlefield Environment Division

ARL-TR-1685

August 1998

NOTICES

Disclaimers

The findings in this report are not to be construed as an official Department of the Army position unless so designated by other authorized documents.

Citation of manufacturer's or trade names does not constitute an official endorsement or approval of the use thereof.

REPORT DOCUMENTATION PAGE

Form Approved
OMB No. 0704-0188

1. AGENCY USE ONLY (Leave Blank)	2. REPORT DATE	3. REPORT TYPE AND DATES COVERED
	August 1998	Final

4. TITLE AND SUBTITLE

The Battlescale Forecast Model (BFM) during the TFXXI at Fort Irwin, CA: Statistical Evaluation of 24 h Forecast Fields and Model Improvement

5. FUNDING NUMBERS

6. AUTHOR(S)

Teizi Henmi, Robert E. Dumais, Jr.

7. PERFORMING ORGANIZATION NAME(S) AND ADDRESS(ES)

U.S. Army Research Laboratory
Information Science & Technology Directorate
Battlefield Environment Division
ATTN: AMSRL-IS-EW
White Sands Missile Range, NM 88002-5501

8. PERFORMING ORGANIZATION REPORT NUMBER

ARL-TR-1685

9. SPONSORING/MONITORING AGENCY NAME(S) AND ADDRESS(ES)

U.S. Army Research Laboratory
2800 Powder Mill Road
Adelphi, MD 20783-1145

10. SPONSORING/MONITORING AGENCY REPORT NUMBER

ARL-TR-1685

11. SUPPLEMENTARY NOTES

12a. DISTRIBUTION/AVAILABILITY STATEMENT

Approved for public release; distribution unlimited.

12b. DISTRIBUTION CODE

A

13. ABSTRACT (Maximum 200 words)

The U.S. Army's Battlescale Forecast Model (BFM) was operationally used for forecasting surface meteorological parameters during the Department of Defence (DOD) Task Force XXI exercise which was held at the National Training Center (NTC), Ft. Irwin, CA, in March 1997.

The results of the BFM forecast calculations were unsatisfactory, primarily due to the following physical and numerical shortcomings in the model operation: scarcity of input meteorological data, poor selections of surface albedo and soil heat conductivity values, nudging method used to assimilate large scale meteorological data dominating the solutions of the equations of motion.

After the exercise, an attempt was made to improve the model's performance. Forecast data, obtained by using different input and boundary condition data and an improved model numerical scheme, were statistically compared with surface automated data collected at the NTC during March 1997.

Using the updated numerics in addition to an upgraded grid distribution of the Navy Operational Global Atmospheric System (NOGAPS) forecast data from 2.5 to 1^{c} resolution (used to provide the large scale forcing for the BFM) resulted in a substantial improvement in the model's forecast skill.

14. SUBJECT TERMS

BFM, mesocale, forecast

15. NUMBER OF PAGES

65

16. PRICE CODE

17. SECURITY CLASSIFICATION OF THIS REPORT	18. SECURITY CLASSIFICATION OF THIS PAGE	19. SECURITY CLASSIFICATION OF ABSTRACT	20. LIMITATION OF ABSTRACT
UNCLASSIFIED	UNCLASSIFIED	UNCLASSIFIED	SAR

NSN 7540-01-280-5500

Standard Form 298 (Rev. 2-89)
prescribed by ANSI Std. Z39-18-298-102

Preface

This report describes the improvements made on the U.S. Army's Battlescale Forecast Model (BFM), based on the experiences from operational use of the model during Task Force XXI exercise, which was held at the National Training Center (NTC), Ft. Irwin, CA, in March 1997.

BFM is now the major part of the U.S. Army's IMETS software, and used regularly for 24-hour forecast over several different regions.

Contents

Figures

Tables

Executive Summary

Introduction

The Battlescale Forecast Model (BFM) was developed at the U.S. Army Research Laboratory (ARL). The BFM was used operationally to forecast boundary layer weather during the Task Force XXI exercise (TFXXI) at the National Training Center (NTC), Fort Irwin, CA. The results of the BFM forecast calculation were unsatisfactory due to physical and numerical shortcomings in the model operation. After the exercise, the model's numerical schemes were modified to improve the model's performance.

Purpose

The purpose of this report is to describe physical and meteorological causes for the sub-par performances of the BFM at NTC, including recent corrections of the BFM performances at NTC before and after the corrections.

Overview

Unsatisfactory results are primarily due to the following physical and numerical shortcomings in the model operation:

- Scarcity of input meteorological data.
- Poor selections of surface albedo and soil heat conductivity values.
- Nudging method used to assimilate large scale meteorological data dominating the solutions of the equations of motion.

After the TFXXI, in an attempt to improve the model's performance, forecast data obtained by using different input and boundary condition data and an improved model numerical scheme were statistically compared with surface automated sensor data collected at the NTC during March 1997. Based on this study, it is concluded that the updated numerics used in addition to an upgraded grid distribution of the NOGAPS forecast data from 2.5° to 1° resolution (used to provide the large scale forcing for the BFM) resulted in substantial improvement in the model's forecast skill.

The present study also shows that the BFM on a model domain with 2.5 km grid spacing is capable of producing reliable forecast results.

1. Introduction

The Battlescale Forecast Model (BFM), developed at the U.S. Army Research Laboratory (ARL), was used operationally to forecast boundary layer weather during the Task Force XXI exercise (TFXXI). [1] TFXXI was held in March 1997 at the National Training Center (NTC), Fort Irwin, CA.

During TFXXI, the BFM was used in various configurations with different grid spacings and model domain sizes. However, the BFM did not perform as well as expected. Notable shortcomings of the model prediction were:

- amplitudes of the diurnal variation of surface temperature were not as large as observed,
- terrain effects on diurnal variation of wind direction were suppressed beyond the 12 h forecast time, and
- surface wind speed during high wind conditions was lighter than observed.

This report describes the physical and meteorological causes for the sub-par performances of the BFM at NTC as well as recent corrections made to improve the BFM performance. This report also gives statistical comparisons of the BFM performances at NTC both before and after the corrections. In TFXXI, the BFM was most frequently used with a model configuration of 21 by 21 horizontal grid points with a grid spacing of 2.5 km (a model domain of 50 by 50 km). All of the BFM calculations in this study were done using this particular configuration. Thus, the feasibility of the BFM application to a model domain with 2.5 km grid spacing (rarely used until this time) will be shown. Figure 1 shows the location of the NTC model domain.

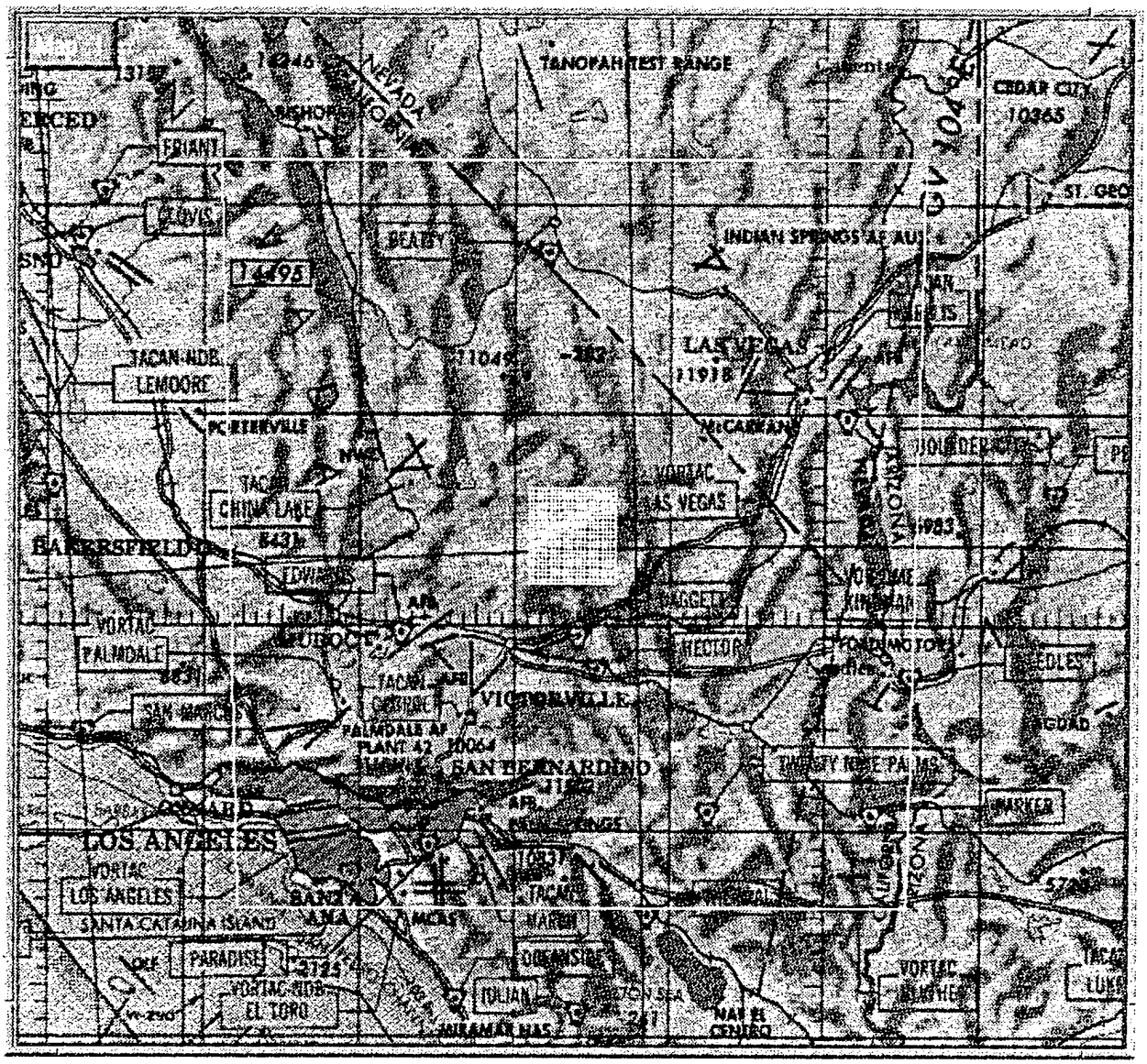

Figure 1. BFM model domain, where the large square used for upper air data collection covers an area of 400 by 400 km, and the gridded square (the BFM domain) covers an area of 50 by 50 km. The center of the model domain is located at 35.417° N and 116.625° W.

2. Causes of Unexpected Performances of the BFM and Improvements Made

This section discusses the major reasons why the version of the BFM operated at NTC produced unsatisfactory results and describes the corrections made to improve the BFM's forecast skill.

2.1. Scarcity of Input Met Data for Initialization and Time-Dependent Boundary Conditions

Currently, the U.S. Air Force Global Weather Center (AFGWC) receives the Navy Operational Global Atmospheric Prediction System (NOGAPS) analysis and forecast data generated by the U.S. Navy Fleet Numerical Meteorological and Oceanographical Center (FNMOC). NOGAPS data are originally calculated horizontally at a 1° resolution grid over the entire globe, and vertically at every mandatory level (1000, 925, 850, 700, 500, 400, 300, 250, 200, 150, 100, 70, 50, 30, and 10 mb) and at selected heights above ground level. In order to utilize old software developed for the U.S. Air Force Global Spectral Model (GSM), AFGWC reduces NOGAPS data horizontally to 2.5° grid spacing and vertically to 1000, 850, 700, 500, 300, and 200 mb.

During TFXXI, the BFM used NOGAPS data from AFGWC and conventional upper air and surface meteorological data. All data were obtained from AFGWC through the Automated Weather Data System (AWDS).

Figure 2 shows NOGAPS (G) and upper air sounding (U) data locations in a 400 by 400 km area centered at 116.625° W and 35.417° N. The inner square represents the BFM model domain area of 50 by 50 km. In the BFM operation, upper air and NOGAPS data available in the outer square are used to produce three-dimensional data fields for initialization and time-dependent boundary values. For this model configuration, input data were scarce, with only two NOGAPS data and one upper air sounding data available.

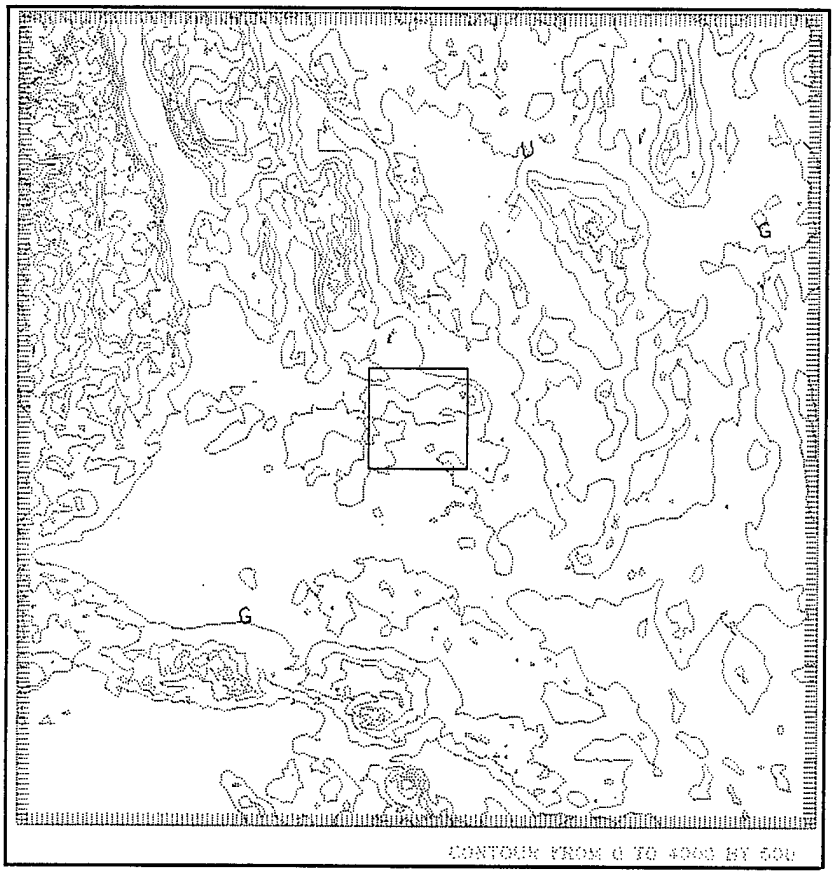

Figure 2. Locations of NOGAPS and upper air sounding data used for the BFM operated at NTC during TFXXI. "G" represents the location of NOGAPS grid points and "U" the location of an upper air sounding site. The entire area covers 400 by 400 km, whereas the inner box (the BFM area) covers 50 by 50 km.

Figure 3 shows the NOGAPS data points with the full 1° grid spacing over the same area. During TFXXI, surface automated meteorological stations (SAMS) were operational at NTC, and the data were archived. The locations of the SAMS are shown in figure 4.

The 1° resolution NOGAPS and SAMS data are used in this study as input data to the BFM, and the results are compared with those of the BFM operated at NTC with the 2.5° resolution NOGAPS input data.

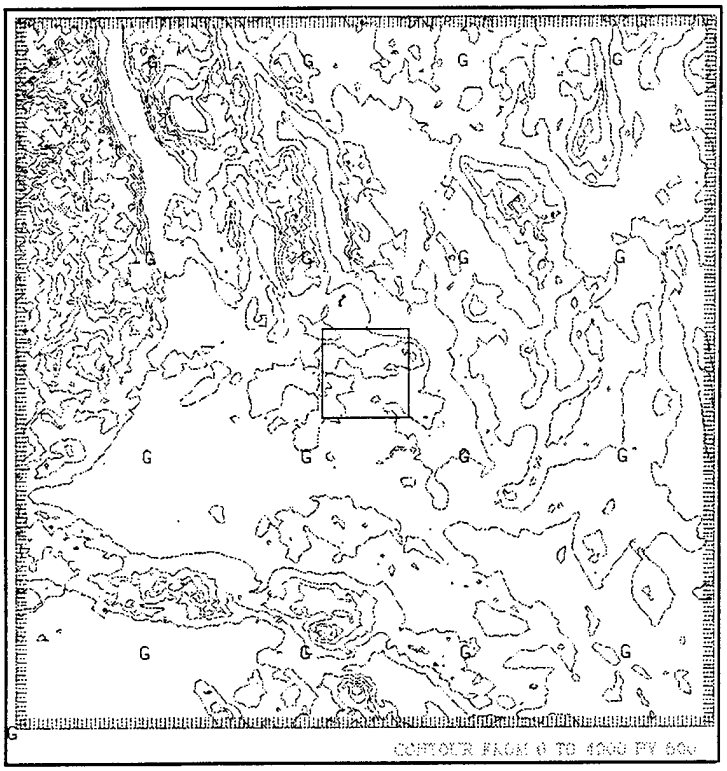

Figure 3. Grid points of NOGAPS data with 1° grid spacing over the model domain. "G" represents the grid point location.

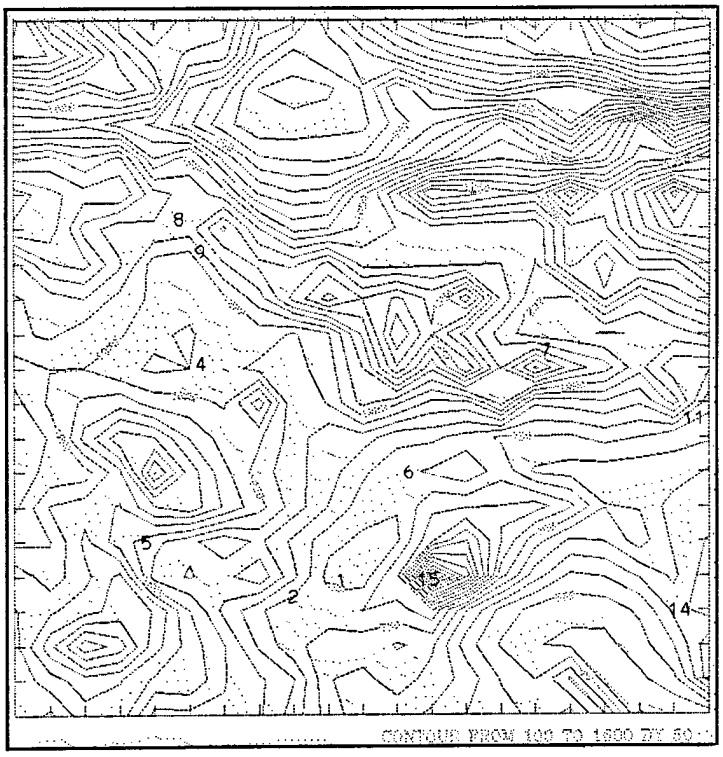

Figure 4. Locations of the SAMS sites in the BFM model domain (50 by 50 km). Numbers represent the locations. There were 11 sites within the model domain.

2.2 Improper Selections of the Values of Surface Albedo and Specific Heat Capacity of Soil

Surface air temperatures obtained by the BFM at NTC showed smaller diurnal variations than observed, and in particular, diurnal maximum temperatures were lower than observed. In obtaining these results, default values for surface albedo and specific heat capacity of soil were set to the constants 0.30 and 1100 $Jkg^{-1}K^{-1}$, respectively. In order to take the soil characteristics into account following Pielke, these two soil parameters are now expressed as a function of both geographical location and time of the year in the BFM's initialization routines. [2] For the NTC area, the albedo value is chosen as 0.175 and the specific heat capacity of soil as 800 ($Jkg^{-1}K^{-1}$). As can be seen in sections 3 and 4, these modifications improved the BFM's forecast skill of the surface temperature field.

2.3 Improper Nudging Method of Meteorological Parameters in the Boundary Layer

The BFM at NTC did not produce diurnal variations of the wind field over complex terrain as expected. In the BFM, the equation of motion for the zonal component of wind is written as:

$$\frac{DU}{Dt} = f(V - V_g) + g\frac{\overline{H} - z^*}{\overline{H}}\left(1 - \frac{<\theta_v>}{\theta_v}\right)\frac{\partial z_g}{\partial x} + \frac{\partial}{\partial x}\left(K_x \frac{\partial U}{\partial x}\right) + \frac{\partial}{\partial y}\left(K_{xy} \frac{\partial U}{\partial y}\right) + \frac{\overline{H}}{H - z_g}\frac{\partial}{\partial z^*}(-\overline{uw}) = C_n(U_t - U) \quad (1)$$

where

C_n = the nudging coefficient
f = the Coriolis parameter
H = the material surface top of the model in z coordinate
$\overline{H}$ = the material surface top of z* coordinate
K_x = the horizontal eddy diffusivity in x direction
K_{xy} = the horizontal eddy diffusivity in xy direction
U = the east-west component of horizontal wind vector
U_t = the east-west component of target wind vector
u = the fluctuation of east-west wind component
w = the fluctuation of vertical wind component
z_g = the ground elevation, and
θ_v = the fluctuation of virtual potential temperature.

In the above expression, $<\theta_v>$ is the base state virtual potential temperature, which is defined as the initial virtual potential temperature obtained by the three-dimensional objective analysis of input data. Details of the BFM equations can be found in Henmi and Dumais. [1] In the BFM version used at NTC, because of the large magnitude of the assigned nudging coefficient (0.0005), the nudging term became so dominant that the terrain effect expressed by the second term of the right-hand side of eq. (1) was masked. Therefore, the wind field within the boundary layer became numerically stagnant due to the damping effect of the nudging term, and the diurnal variation of the boundary layer wind was not produced. In order to correct for the masking effect, the nudging term was removed from all numerical calculations for the vertical layers within 150 m of the ground when the large-scale flow was weak (defined as where the NOGAPS forecast wind speeds at all levels below 1000 m above sea level were >10 m/s). This is not applied during the initialization process in which the BFM fields are dynamically nudged toward the three-dimensional data fields generated from NOGAPS, upper air, and the surface observed data. During weak large-scale flow, it is assumed that meteorological fields in the boundary layer are mainly dominated by surface exchanges of temperature, moisture, and momentum.

In order to solve the problem in which the BFM surface forecast of wind speeds were smaller than observed during the periods of strong wind speed, the horizontal wind vector components of the model in the layers between the surface to 1000 m level are nudged to the wind vector components at the 1000 m level of the input data if the following criteria are met: (1) the maximum wind speeds of NOGAPS data at any level from the surface to 1000 m is greater than 10 m/s; (2) the difference of the NOGAPS wind direction between 10 and 1000 m is smaller than 35°; and (3) the solar radiation intensity is greater than 300 W/m^2. Under this approach, it is assumed that the combination of strong winds and a well-mixed boundary layer leads to uniform wind vectors in the boundary layer. Panofsky et al., derived the following relationship for wind speed as a function of height: [3]

$$V_2 = V_1\left(\frac{z_2}{z_1}\right)^{\alpha} \tag{2}$$

where

V_1 = the wind speed at height z_1
V_2 = the wind speeds height z_2, and
α = the equivalent power law exponent, given analytically by

$$\alpha = \frac{\phi\left(\frac{z_g}{L}\right)}{\ln\left(\frac{z_g}{z_0}\right) - \psi\left(\frac{z_g}{L}\right)} \tag{3}$$

where

$z_g = (z^1 z^2)^{1/2}$ and

ϕ and ψ = universal functions of height z_g, relative to the similarity scale (Monin-Obukhov length).

For the atmospheric stability conditions between neutral and unstable ranges, the value of α varies from 0.06 to 0.13 for the roughness length $Z_0 = 0.1$ m. [4] From the above relationship, for $V_1 = 10$ m/s at $z_1 = 1000$ m, the wind speed at the 10 m level, V_2, ranges between 5.5 and 7.6 m/s. Therefore, our assumption above may slightly overestimate the wind speed. Unfortunately, in the present study, there is no case with the wind speed greater than 10 m/s at 1000 m level; therefore, the validity of our approach must be examined in the future.

3. Statistical Evaluation of Model Performance

In the following sections, "old" BFM is defined as the BFM used at NTC for TFXXI, and "new" BFM is as described in section 2. NOGAPS data used for this study are obtained through the Internet homepage of the Master Environmental Library (MEL), whose address is:

http://www-mel.nrlmry.navy.mil/homepage.html.

The data are available at every 1° point over the entire earth, as shown in figure 3. As can be seen from figure 3, while the present study's BFM domain does not include any NOGAPS grid points, the number of grid points over the 400 by 400 km area is larger than for the old BFM.

In this report, surface temperature, wind speed, and horizontal wind vector components (u and v), are used for the comparison study. The moisture data archived were in the form of relative humidity at sea level; hence, they were not suitable for the present study.

Surface observed data covering 16 through 25 March 1997 are compared with forecast data. Unfortunately, there was no high surface wind case during this period; hence, the model improvement designed to be incorperated with high surface-wind speed conditions could not be tested in this study.

The 24 h forecast datasets of the above variables are statistically compared with surface data observed at 11 sites located in the model domain of 50 by 50 km (see figure 4).

3.1 Simulation Datasets in the Study

(1) Archived Data of Old BFM Operated at NTC (OB)

During the TFXXI exercise, output files of the BFM forecast calculations were archived. The BFM's initialization data were provided by two NOGAPS grid points from AFGWC, one conventional upper air sounding site, and one surface observation site, shown in figure 2. Time-dependent boundary condition data were supplied by two NOGAPS grid points and were spatially and temporally interpolated onto the BFM domain. The NOGAPS 12 h forecast fields were used for the BFM initialization, while the NOGAPS 24 and 36 h forecast fields were used to provide the BFM's 12 and 24 h boundary conditions, respectively.

(2) 1° NOGAPS Data Interpolated Spatially and Temporally to the Model Domain (NG)

The 1° NOGAPS data valid for the forecast times of 0, 12, and 24 h were spatially and temporally interpolated to the BFM model domain and compared with the surface observation data.

(3) Old BFM Data Obtained by Using 1° NOGAPS Data and Surface Data for Initialization (OB + NG + S)

The 1° NOGAPS data and surface observation data shown in figure 3 are used to initialize the old BFM. The time-dependent boundary values were supplied by nudging to the NOGAPS data. Upper air sounding data was not used.

(4) New BFM Data Obtained by Using Only 1° NOGAPS Data for Initialization (NB + NG)

The new BFM was initialized using only 1° NOGAPS data, and time-dependent boundary values were given by nudging towards the NOGAPS fields as in *(1)* and *(3)*. Raw surface and upper air observations were not used in the initialization.

(5) New BFM Data Obtained by Using NOGAPS Data Plus Surface Observation Data for Initialization (NB + NG + S)

The new BFM was initialized by using 1° NOGAPS data plus surface observation data, while NOGAPS data provided time-dependent boundary values by way of nudging, as in *(1)*, *(3)*, and *(4)*. Upper air sounding data was not used in the initialization.

From the comparison between *(4)* and *(5)*, the effects of utilization of surface observation data for initialization can be seen. From the comparison between *(3)* and *(5)*, the skills of the old and new BFMs can be distinguished. Comparisons between *(2)* and *(4)* or *(5)* make it possible to examine the influence of the NOGAPS over the BFM. In the following sections, these five sets are represented by *(1)*, *(2)*, etc.

3.2 Statistical Parameters

The following statistical parameters between forecast data and surface observed data are calculated using the data obtained for the period from 16 through 25 March 1997.

1. Mean Difference

$$MD = \frac{\sum_{i=1}^{n}\left(x_{o,i} - x_{p,i}\right)}{n} \tag{4}$$

Here, the subscripts $_o$ and $_p$ represent observation and prediction, respectively. The subscript $_i$ represents the i^{th} observation point, and n is the total number of observations.

2. Mean Absolute Difference

$$AD = \frac{\sum_{i=1}^{n}\left|x_{o,i} - x_{p,i}\right|}{n} \tag{5}$$

3. Root Mean Square Error

$$\sigma = \sqrt{\frac{\sum_{i=1}^{n}\left(x_{o,i} - x_{p,i}\right)^2}{n}} \tag{6}$$

4. Correlation Coefficient

$$R = \frac{\sum_{i=1}^{n}\left[\left(x_{o,i} - \bar{x}_o\right)\left(x_{p,i} - \bar{x}_p\right)\right]}{\sqrt{\sum_{i=1}^{n}\left(x_{o,i} - \bar{x}_o\right)^2 \sum_{i=1}^{n}\left(x_{p,i} - \bar{x}_p\right)^2}} \tag{7}$$

where x_o and x_p are the mean values of observation and forecast data, respectively.

Among these four parameters, better agreements between observation and forecast are, in general, related to smaller values of AD and σ, and larger values of the correlation coefficient, R. A nonzero MD indicates bias.

3.3 Statistical Comparisons for Each Surface Observation Site

The four statistical parameters described above were calculated for each site, and the results at 0, 3, 6, 9, 12, 18, and 24 h were combined. Tables 1(a), (b) and (c) show the statistics for temperature. The mean absolute difference, correlation coefficient, and mean difference are given in (a), (b), and (c), respectively.

Table 1. Mean absolute difference (°C), correlation coefficient, and mean difference (°C) for temperature

(a) Mean absolute difference

Site	(1) OB	(2) NG	(3) OB+NG+S	(4) NB+NG	(5) NB+NG+S
1. Bike Lake	4.9	3.9	3.3	3.6	3.4
2. 247th Pad	5.0	3.7	3.6	3.8	3.8
4. Nelson Lake	4.6	7.0	5.8	5.5	5.5
5. Gold Stone	4.1	1.9	4.9	4.9	4.8
6. Four Corners	5.1	6.5	4.9	4.8	4.7
7. Granite Pass	6.0	8.6	6.9	6.1	6.0
8. Gary Owen	4.5	7.0	6.0	5.6	5.6
9. Live Fire	6.3	6.0	4.5	4.8	4.8
11. East Gate	5.4	6.9	4.9	5.0	5.1
14. Red Pass Lake	8.9	4.2	6.4	6.6	6.6
15. NASA Site	4.7	4.3	3.0	3.2	3.2
Mean	5.4	5.4	4.9	4.9	4.9

(b) Correlation coefficient

Site	(1) OB	(2) NG	(3) OB+NG+S	(4) NB+NG	(5) NB+NG+S
1. Bike Lake	0.37	0.54	0.56	0.57	0.58
2. 247th Pad	0.31	0.51	0.46	0.54	0.56
4. Nelson Lake	0.35	0.43	0.58	0.56	0.57
5. Gold Stone	0.37	0.55	0.57	0.59	0.60
6. Four Corners	0.25	0.29	0.48	0.50	0.50
7. Granite Pass	0.05	0.21	0.40	0.51	0.52
8. GaryOwen	0.28	0.54	0.58	0.58	0.60
9. Live Fire	0.17	0.25	0.46	0.49	0.50
11. East Gate	0.28	0.33	0.52	0.56	0.57
14. Red Pass Lake	0.28	0.61	0.51	0.57	0.59
15. NASA Site	0.38	0.52	0.56	0.57	0.58
Mean	0.26	0.43	0.52	0.55	0.56

Table 1. Mean absolute difference (°C), correlation coefficient, and mean difference (°C) for temperature (continued)

(c) Mean difference

Site	(1) OB	(2) NG	(3) OB+NG+S	(4) NB+NG	(5) NB+NG+S
1. Bike Lake	-3.7	3.0	0.6	0.6	0.6
2. 247th Path	-3.6	2.2	0.1	-0.4	-0.3
4. Nelson Lake	1.6	6.6	5.1	4.4	4.5
5. Gold Stone	.4	5.9	4.0	3.8	3.9
6. Four Corners	-1.8	4.6	2.6	1.9	1.9
7. Granite Pass	1.1	6.2	4.7	3.3	3.3
8. Gary Owen	1.4	7.0	5.5	5.0	5.0
9. Live Fire	-2.6	3.2	1.8	0.9	0.9
11. East Gate	-2.0	3.3	2.0	0.8	0.9
14. Red Pass Lake	-8.9	-3.6	-6.0	-6.2	-6.1
15. NASA Site	-2.4	2.9	0.6	0.4	0.4
Mean	-1.86	3.5	1.9	1.3	1.3

Table 1(c) is for each observation site and for datasets (1) through (5). Here, only mean absolute difference, correlation coefficient, and mean difference are presented because absolute difference and root-mean square error show similar tendencies.

From table 1, the following can be inferred:

1) NOGAPS with 1° gridspacing [dataset (2)], even without using the BFM, produced better correlationship in temperature than the old BFM operated at NTC [dataset (1)].

2) The old BFM with 1° NOGAPS data produced further improved surface temperature fields. Boundary layer physics in the BFM have produced diurnal variation of surface temperature fields, resulting in an improved correlation between observation and forecast.

3) From the comparison between datasets (3) and (5), a slight, but not substantial, improvement of surface temperature fields by running the new BFM over the old BFM is noticed.

4) By comparing datasets (4) and (5), it is seen that the use of surface observation data for initialization did not produce noticeable improvement in the statistics of surface temperature fields.

5) There appears to be sites exhibiting consistent biases in temperature, most notably site 14 (Red Pass Lake). The temperature recorded at site 14 was probably lower than the actual temperature. Figure 5 shows average temperatures and standard deviations for the period of TFXXI, as plotted against the site elevations. Surface temperature is dependent upon many physical factors including elevation, but site 14 seems to have recorded temperatures lower than truth.

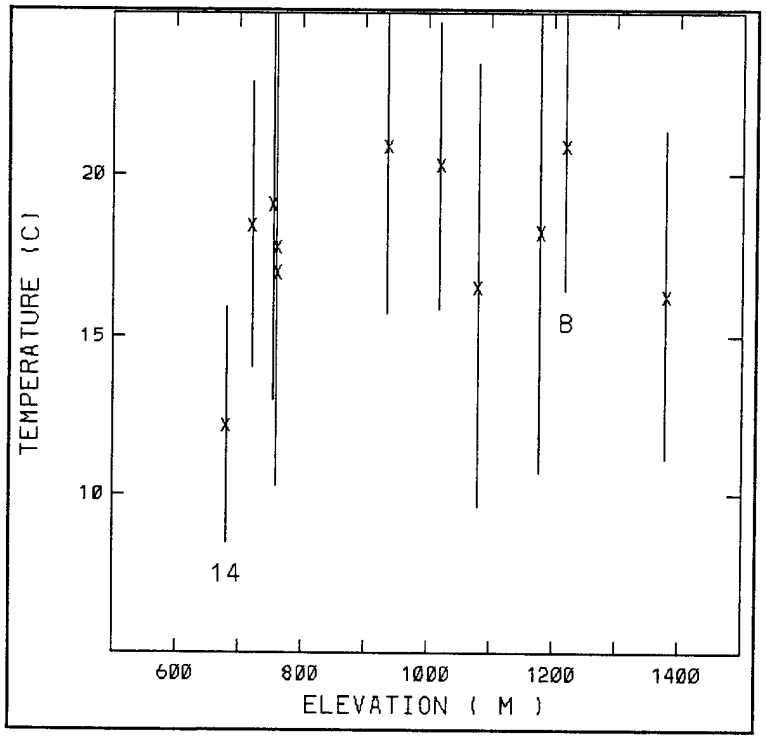

Figure 5. Means and standard deviations of surface temperature during TFXXI, plotted against elevations of observation sites.

6) Mean difference values for dataset (2) are greater than zero for all sites except 14, indicating that NOGAPS-predicted surface temperature fields are lower than observed temperature fields over the model domain during TFXXI exercise period.

7) Datasets (4) and (5) yielded the best statistical agreement among the five datasets. However, the use of surface temperature data for initialization produced little improvement in the values of statistical parameters. Surface temperature fields forecast by the BFM may be predominantly influenced by those of NOGAPS. Nudging of observed surface temperature during the initialization process also produced little differences. Further study will be needed to identify the cause or causes of these differences.

Tables 2 (a), (b), and (c) show similar statistics for wind speed. Dataset (5), produced by the new BFM using NOGAPS data with 1° grid spacing, showed the best statistical results among the five datasets. All three statistical parameters show the best performance by dataset (5). Significantly improved statistical values are obtained by dataset (3) over (1), indicating that input data for initialization and boundary values are important. Dataset (5) showed substantially better statistical values over datasets (3) and (4), indicating that the new BFM with better input data has produced better forecast fields of wind speed. The improvements of statistical values of data set (5) over (4) are due to the use of surface data for initialization.

Table 2. Mean absolute difference (m/s), correlation coefficient, and mean difference (m/s) for wind speed

(a) Mean absolute difference

Site	(1) OB	(2) NG	(3) OB+NG+S	(4) NB+NG	(5) NB+NG+S
1. Bike Lake	3.6	3.2	2.6	2.6	2.2
2. 247th Pad	3.2	2.7	2.2	2.3	1.9
4. Nelson Lake	3.5	2.7	2.1	2.2	2.0
5. Gold Stone	2.9	3.4	2.3	2.7	2.3
6. Four Corners	2.0	2.5	2.1	2.2	2.0
7. Granite Pass	1.9	2.0	1.6	1.7	1.4
8. Gary Owen	2.2	2.5	2.3	2.4	2.2
9. Live Fire	2.7	3.0	1.9	2.3	2.1
11. East Gate	2.8	2.4	2.3	1.9	1.6
14. Red Pass Lake	3.1	3.3	2.8	3.2	2.6
15. NASA Site	2.5	2.0	2.3	2.1	1.8
Mean	2.7	2.7	2.2	2.3	2.0

(b) Correlation coefficient

Site	(1) OB	(2) NG	(3) OB+NG+S	(4) NB+NG	(5) NB+NG+S
1. Bike Lake	-0.10	-0.16	0.19	0.14	0.24
2. 247th Pad	0.26	0.05	0.32	0.20	0.35
4. Nelson Lake	-0.01	0.05	0.14	0.20	0.33
5. Gold Stone	-0.09	-0.15	0.19	0.22	0.35
6. Four Corners	0.17	0.01	0.13	0.14	0.27
7. Granite Pass	0.03	0.20	0.32	0.34	0.48
8. GaryOwen	0.16	0.00	0.15	0.12	0.25
9. Live Fire	-0.04	0.07	0.35	0.30	0.44
11. East Gate	0.09	-0.08	0.22	0.17	0.20
14. Red Pass Lake	0.19	0.17	0.12	-0.03	0.24
15. NASA Site	0.14	0.21	0.37	0.25	0.33
Mean	0.07	0.03	0.23	0.19	0.32

Table 2. Mean absolute difference (m/s), correlation coefficient, and mean difference (m/s) for wind speed (continued)

(c) Mean difference

Site	(1) OB	(2) NG	(3) OB+NG+S	(4) NB+NG	(5) NB+NG+S
1. Bike Lake	3.3	0.7	1.9	1.4	1.0
2. 247th Path	2.8	1.1	1.6	1.1	0.7
4. Nelson Lake	3.1	0.4	0.4	0.3	0.1
5. Gold Stone	2.3	0.5	0.0	-0.4	-0.6
6. Four Corners	1.0	-0.6	-0.3	-0.3	-0.6
7. Granite Pass	0.9	-0.7	0.0	-0.3	-0.5
8. Gary Owen	1.0	-0.2	0.2	0.1	-0.2
9. Live Fire	1.7	0.0	0.0	-0.2	-0.4
11. East Gate	2.1	-0.6	0.8	-0.5	-0.4
14. Red Pass Lake	2.9	2.0	2.4	2.5	2.0
15. NASA Site	2.0	0.3	1.9	1.4	1.0
Mean	2.1	0.3	0.8	0.5	0.2

During the TFXXI exercise, wind speeds forecast by the old BFM were lighter than observed, as can be seen from the values of mean difference for dataset (1), but the values of mean difference for the rest of datasets indicate that the use of NOGAPS data with 1° grid spacing considerably improved the forecast of wind speed.

Unlike temperature and wind speed, the statistics of wind components do not show the improved performances of the new BFM over old BFM (the results are not shown here). Wind component forecast differences between the new and old BFMs will be discussed later.

3.4 Time Dependencies of the Statistical Parameters

Figures 6A through 6D show the time dependencies of the four statistical parameters for surface temperature calculated by using the data of all sites combined (for each dataset). In figures 6A through 6D, (1), (2), (4), and (5) represent the four different datasets. The results for dataset (3) (not shown here) were superior to (2), but inferior to (4). The following can be inferred from figures 6A through 6D:

- Datasets (4) and (5) produced very similar temporal variations in all the parameters. The nudging of observed surface temperature did not produce noticeable improvement in the forecast of surface temperature.

- Datasets (4) and (5) produced better statistical results than (1) and (2) through 18 h, but at the 24 h forecast period, the statistics for (4) and (5) became worse than those of (1) and (2). The combined effects of model physics and nudging of NOGAPS data apparently produced larger values of absolute difference and root-mean square error and smaller values of the correlation coefficient for the 24 h forecast. Note how the statistics at 24 h for dataset (2) show similar tendencies with those for (4) and (5).

- The old BFM operated at NTC produced surface temperature fields that were not well correlated with observation during the first 12 h of the forecast period, due to the shortcomings of the old BFM that were unable to produce diurnal variation of the surface temperature field.

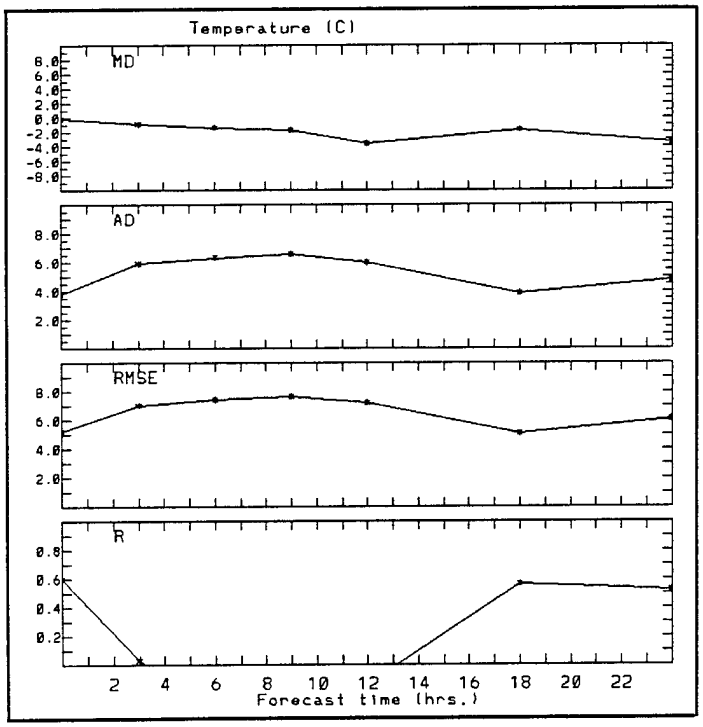

Figure 6A. Time changes of statistical parameters for temperature for dataset (1).

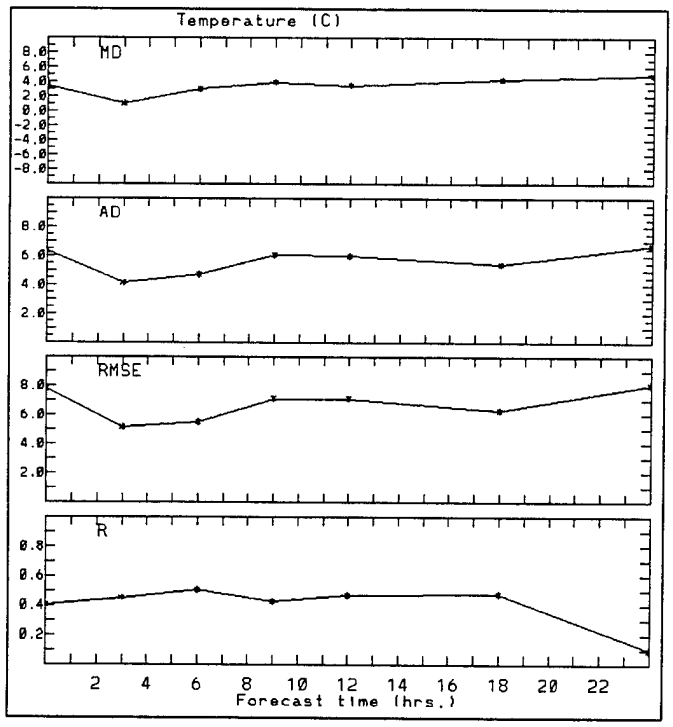

Figure 6B. Same as figure 6A, except for dataset (2).

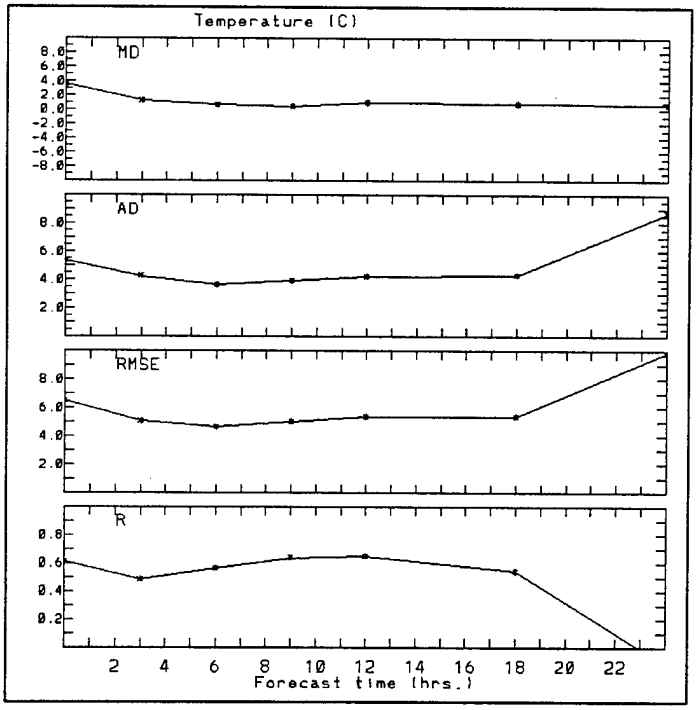

Figure 6C. Same as figure 6A, except for dataset (4).

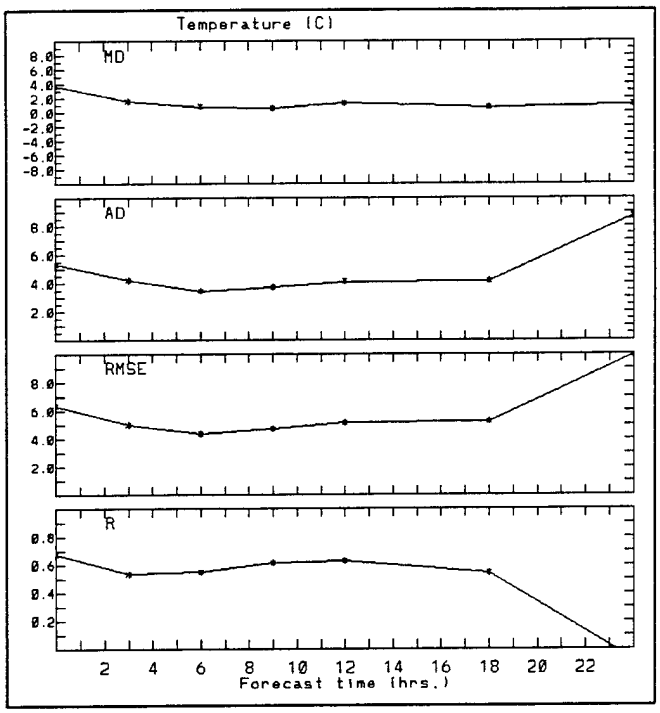

Figure 6D. Same as figure 6A, except for dataset (5).

Time dependencies of the statistical parameters for wind speed are shown in figures 7A through 7D. For wind speed, dataset (5), produced by the new BFM, resulted in the best statistics among the four datasets. The differences between datasets (4) and (5) can be seen during the first 6 h of forecast. Nudging of surface wind data improved surface wind fields in the early hours of the forecast, but after 6 h, the influences of surface wind data nudging seemed to disappear. In the BFM model, the nudging effects of surface data decay by multiplying exp(-kt) to the nudging terms in the surface layers after initialization time. [2] Here, k is an empirical coefficient, and t is the time beginning at the completion of initialization. In effect, the initial value of the nudging coefficient and the empirical damping coefficient k are such that the value of the nudging coefficient damps to an inconsequential value after 6 h.

Datasets (4) and (5) showed substantial improvements in the value of statistical parameters for wind speed over datasets (1) and (2). Similar figures are obtained for wind vector components, u and v, as shown in figures 8A through 8D and 9A through 9D. For the x- component of wind vector, dataset (1) yielded better statistical values in correlation coefficient than did datasets (2), (4), and (5). During the TFXXI exercise, predominant wind direction over the area appears to have been from the west. Under such conditions, there might not have been significant differences in the x- component of the wind vector interpolated from datasets (1), (4), and (5). Further studies are needed to understand why dataset (1) resulted in better statistical values in the correlation coefficient.

Again, the influences of nudging the surface wind data can be seen for wind vector components in the first several hours of forecast run, by comparing time variations of the four statistical parameters for dataset (5) with those of (4).

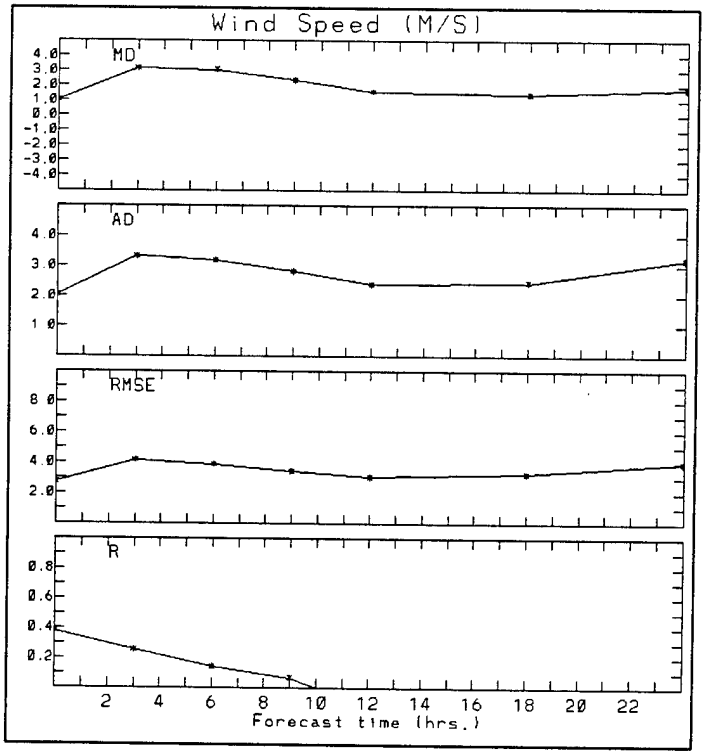

Figure 7A. Time changes of statistical parameters for wind speed for dataset (1).

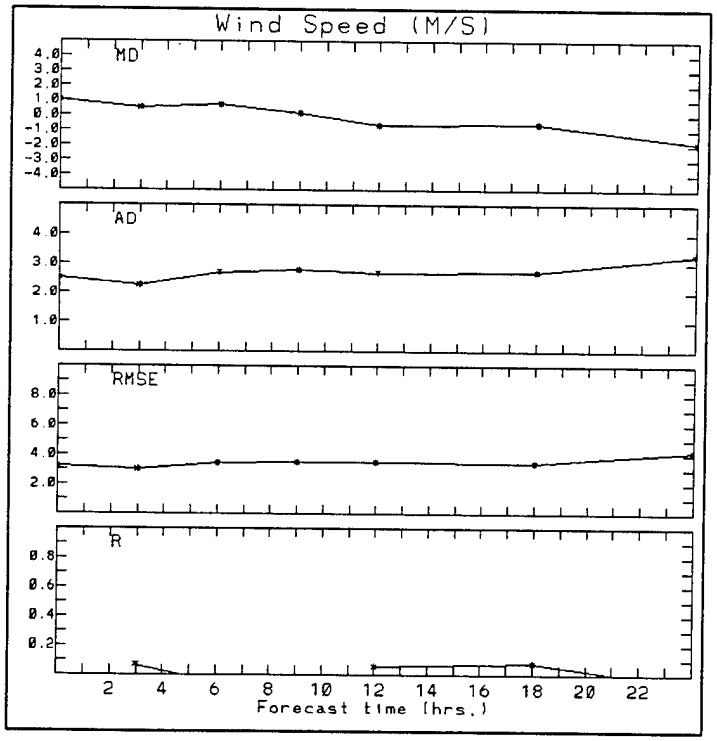

Figure 7B. Same as figure 7A, except for dataset (2).

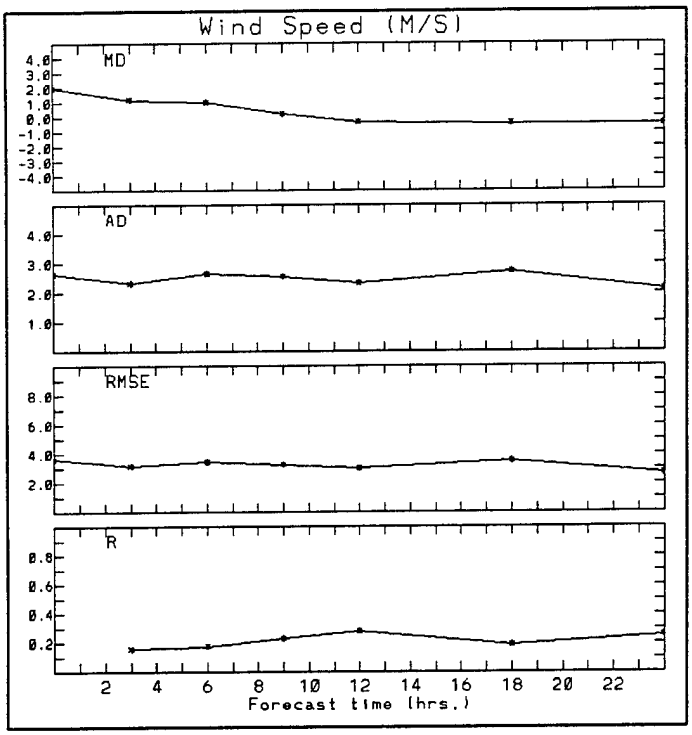

Figure 7C. Same as figure 7A, except for dataset (4).

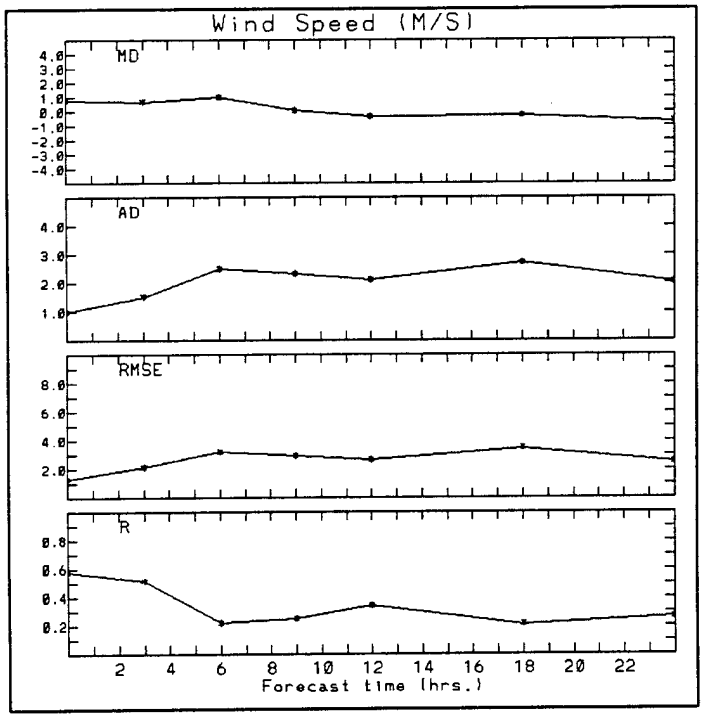

Figure 7D. Same as figure 7A, except for dataset (5).

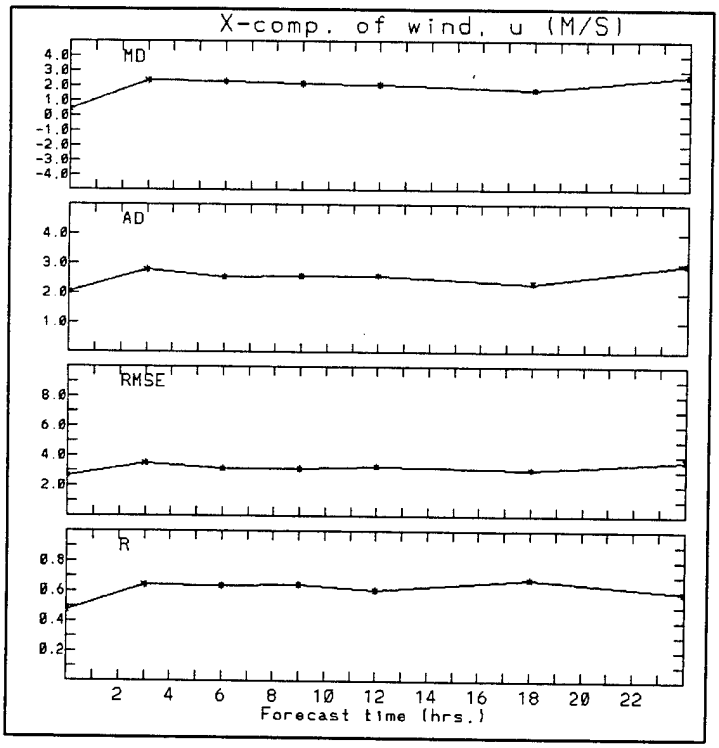

Figure 8A. Time changes of statistical parameters for x- component of wind, u, for dataset (1).

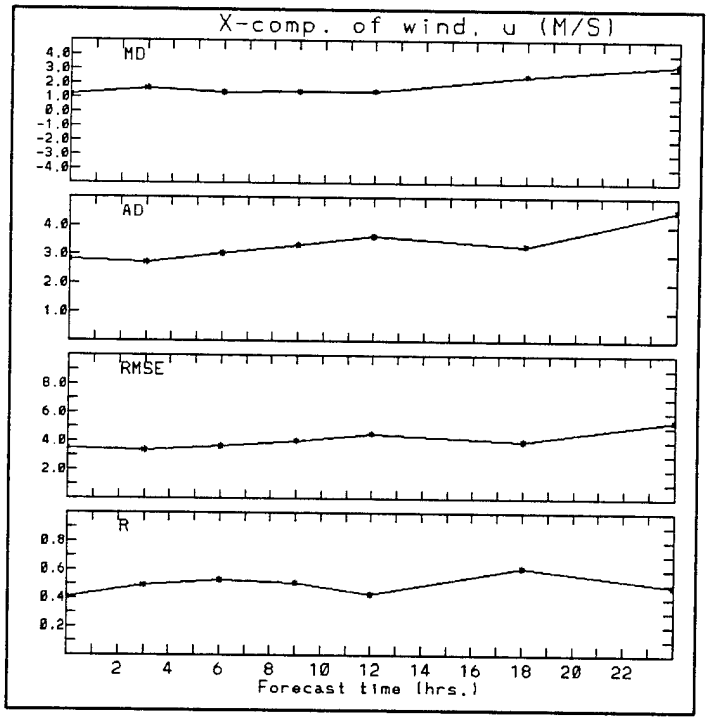

Figure 8B. Same as figure 8A, except for dataset (2).

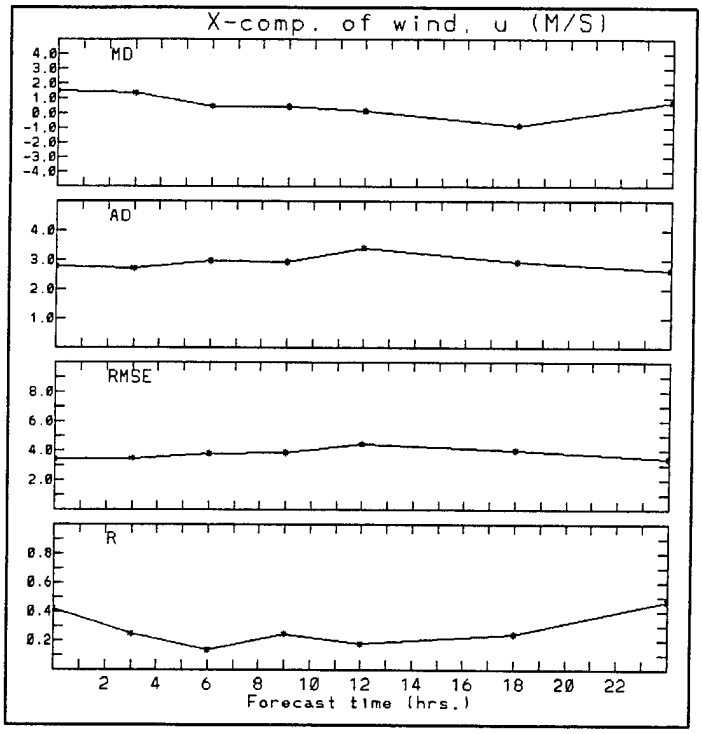

Figure 8C. Same as figure 8A, except for dataset (4).

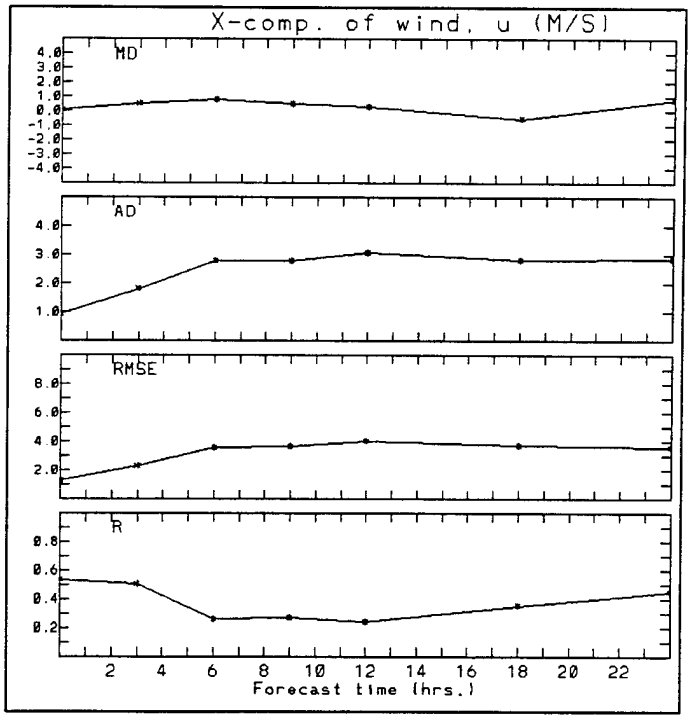

Figure 8D. Same as figure 8A, except for dataset (5).

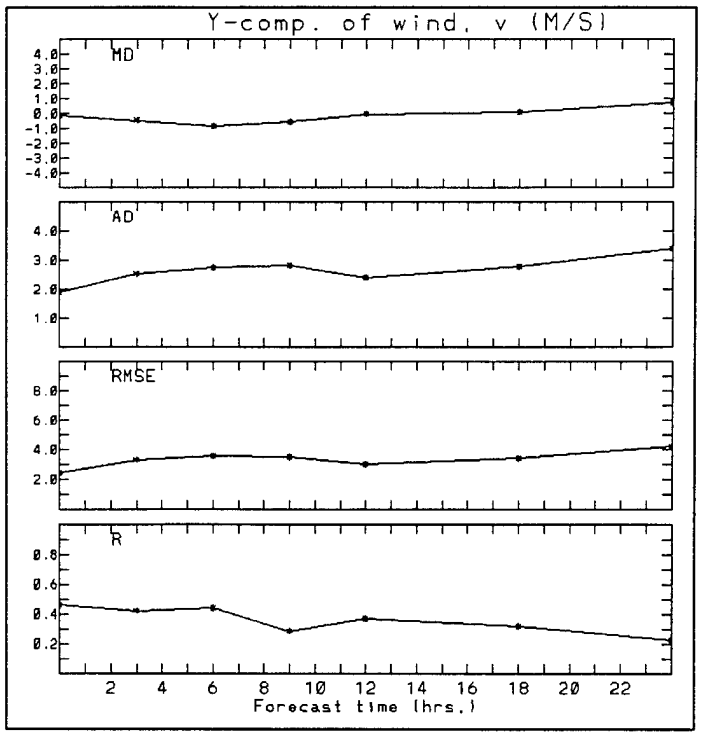

Figure 9A. Time changes of statistical parameters for y- component of wind, v, for dataset (1).

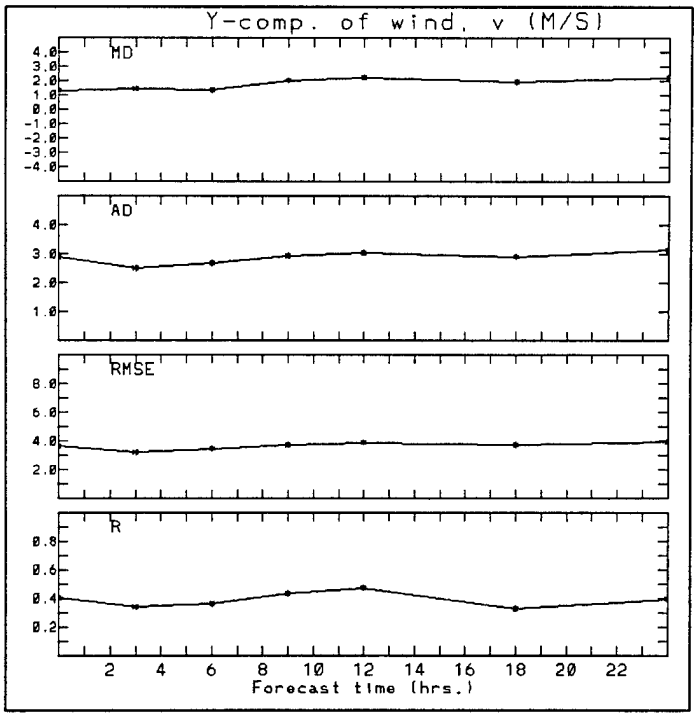

Figure 9B. Same as figure 9A, except for dataset (2).

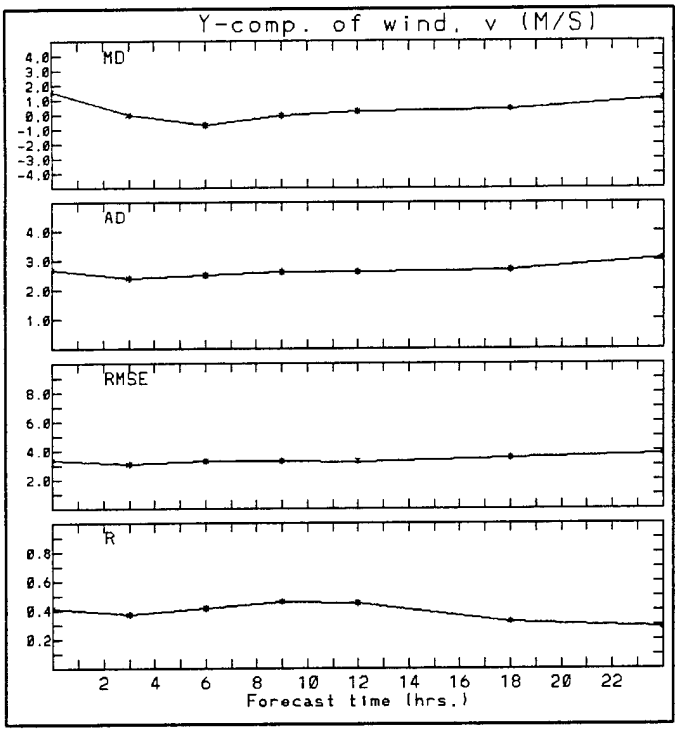

Figure 9C. Same as figure 9A, except for dataset (4).

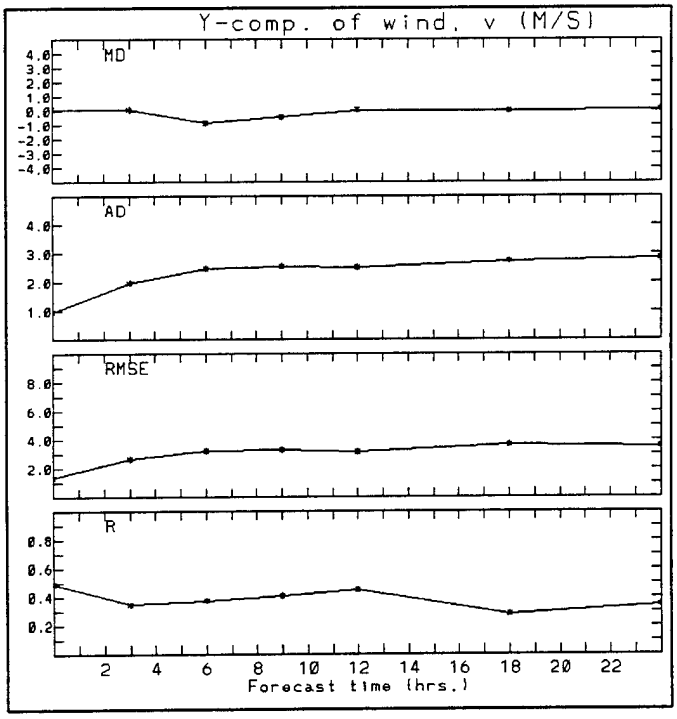

Figure 9D. Same as figure 9A, except for dataset (5).

From these statistical studies, it can be concluded that the new BFM has produced statistically better surface forecast fields in temperature and wind, and that the use of NOGAPS data with 1° grid spacing has substantially contributed to produce these improved fields of temperature and wind.

3.5 Comparisons with Previous Statistical Studies

In previous studies of the BFM, input data for initialization and time-dependent boundary conditions were provided by the GSM. [5,6] The GSM data were given at grid points with 381 km grid spacing, at pressure levels of 1000, 850, 700, 500, 300, and 200 mbs, and at 12 h increments.

Henmi, et al. performed a study over a model domain of 250 by 250 km with 5 km grid spacing, centered on the White Sands Missile Range (WSMR), NM. [5] By comparing forecast results with surface data observed by the WSMR SAMS sites, Henmi, et al. showed that the BFM produced substantially improved forecast fields over a spatial and temporal interpolation of GSM data. [5] Furthermore, it was shown that incorporation of surface data into the initial field improved the forecast fields for several hours after initialization.

The study by Knapp and Dumais was centered at Colorado Springs, CO, with two model domains, the first covering 500 by 500 km with 10 km grid spacing and the second 250 by 250 km with 5 km grid spacing. Comparisons of 12 h forecast data by the model with surface station observation data showed that the BFM was far superior to the GSM model for surface parameters such as wind speed, x- and y- components of the wind vector, temperature, and dew point temperature.

For temperature forecasts, the mean absolute difference values for the period from 0 to 12 h were 3.3 and 3.0° C for the models with 5 and 10 km grid spacings, respectively. The current study shows about 4.1° C for the same period in dataset (5) (see figures 6A through 6D). Dataset (5) represents the data produced by the BFM over a model domain of 50 by 50 km with 2.5 km grid spacing. It is impossible to identify the cause of the inferior results of the current study in temperature forecasting, except that there are some stations recording questionable observations.

For wind speed forecast, the Knapp and Dumais study over Colorado showed that the BFM wind forecasts for the 12 h period produced a mean absolute

difference 42 percent lower than the GSM at both grid spacings. [6] In the current study, the mean absolute difference for the 24 h period by the BFM was 35 percent lower than the NOGAPS data. Also in the Knapp and Dumais study, the mean absolute difference for wind speed by the GSM for the 12 h period was about 4 m/s for both 5 and 10 km grid spacings. [6] The current study showed the mean absolute difference for 24 h period wind speed by the NOGAPS was 2.7 m/s [as shown in table 2 (a) for dataset (2)]. This means that the interpolation to 2.5 km resolution grid points from the NOGAPS with 1° grid spacing has produced better forecasts of wind speed than the interpolation to 5 and 10 km resolution grid points from the GSM with 381 km grid spacing. The reason for better forecast by the current study than that by Knapp and Dumais is probably the use of better initialization and time-dependent boundary conditions by 1° NOGAPS than those by the GSM.

In table 3, the absolute difference values calculated in the present study along with those for the Knapp and Dumais are summarized. [6] The values for the present study were calculated using the data between 0 and 24 h, and those by Knapp and Dumais were calculated using the data between 0 and 12 h. It is also noted that the NOGAPS and the GSM are different models. Therefore, direct comparison should not be made; although, except for temperature, the absolute difference values for wind speed, and u and v are very similar.

Table 3. Comparisons of the mean absolute difference values for temperature, wind speed, and x- and y- components of wind vector. For the current study, the values are calculated for the period between 0 and 24 h, whereas for Knapp and Dumais, they are calculated for the period between 0 and 12 h

Reference	Large-scale model	Grid resolution (km)	Temp. (° C)	Wind speed (m/s)	u (m/s)	v (m/s)
Current study	NOGAPS with 1° spacing	2.5	4.9	2.0	2.4	2.3
Knapp & Dumais	GSM with 381 km spacing	5.0	3.3	1.9	2.5	2.5
Knapp & Dumais	GSM with 381 km spacing	10.0	3.0	1.8	2.3	2.4

4. Comparisons of 24 h Forecast Output with Observation

In this section, examples of the forecast output are presented to show qualitatively the improvements of the new BFM over the old BFM operation at the NTC.

Figures 10A through 10F, respectively, show time variations of temperature, wind speed, and wind direction at three surface observation sites: 14 Red Pass Lake, 15 NASA Site, and 1 Bike Lake (see also figure 4). These figures show both good and bad examples. The results of old BFM operated at NTC are shown on the top part of the pages, and those of new BFM on the bottom part. Thick lines represent forecast values and thin lines observed values. The forecast calculations are made for 19 March 1997, (Julian day = 78). In each figure, the top represents temperature variation, the middle wind speed, and the bottom wind direction. Note that the forecast initialization time for the old BFM in this example is 02Z and that for the new BFM is 00Z, and the results for new BFM are plotted every hour.

The following can be seen from the figures:

- The old BFM operated at the NTC did not produce diurnal variations in temperature and wind direction as much as observed. As has been mentioned, these are due to numerical stagnation caused by nudging in the boundary layer.

- For the new BFM forecast calculations, the temperature deviations from observation are introduced initially and have lasted throughout the forecast period. In the present study, the forecast values for the surface observation sites were given by those of the nearest grid point. The differences of altitudes between those interpolated from the elevation data and those measured are as follows:

	Interpolated (m)	Measured (m)	Difference (m)
1 Bike Lake	729.0	720.0	+9.0
11 NASA Site	1326.0	1380.0	-54.0
14 Red Pass Lake	614.0	680.0	-66.0

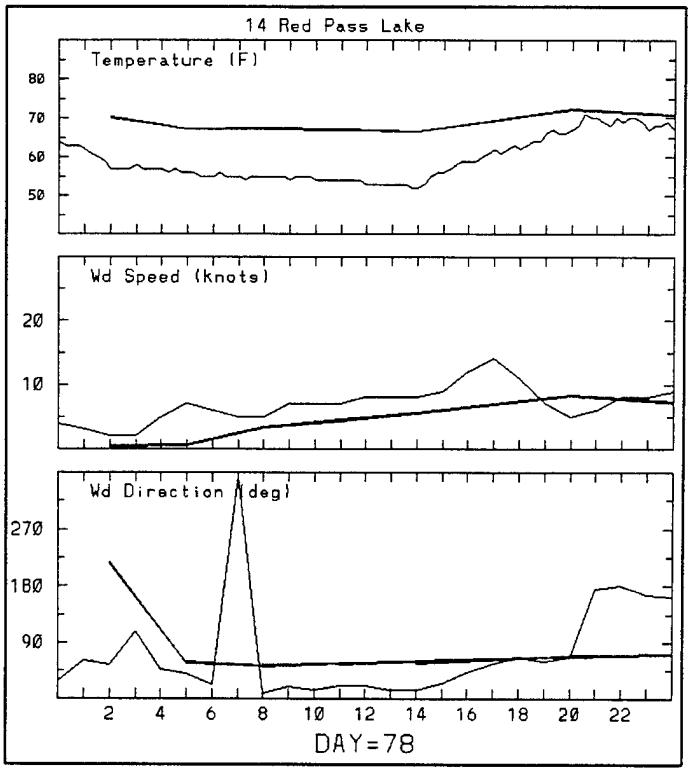

Figure 10A. Time variations of surface temperature, wind speed, and direction. Thick lines represent forecast calculation and thin lines observation. The results of the old BFM at NTC for Red Pass Lake (14) are shown.

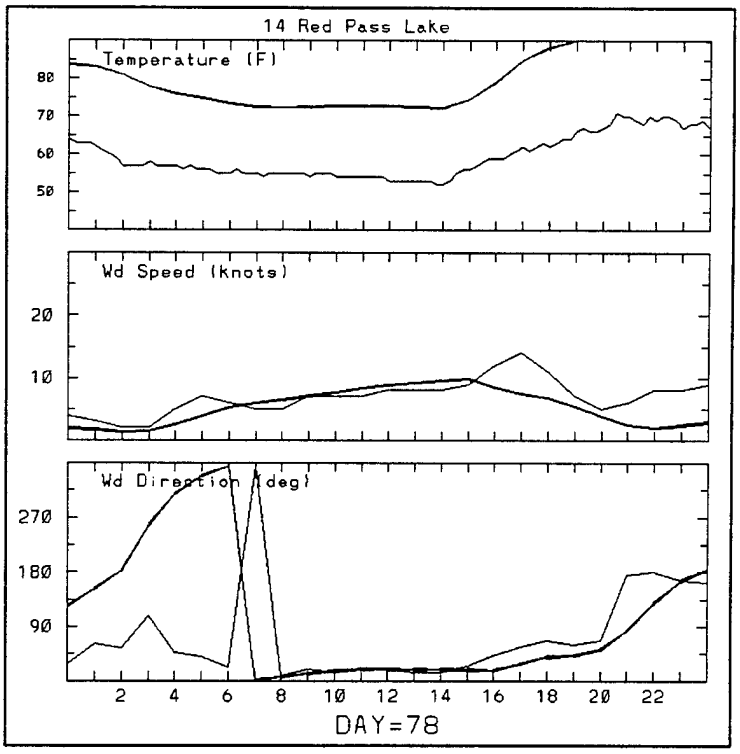

Figure 10B. Same as figure 10A, except for the results of the new BFM for Red Pass Lake (14).

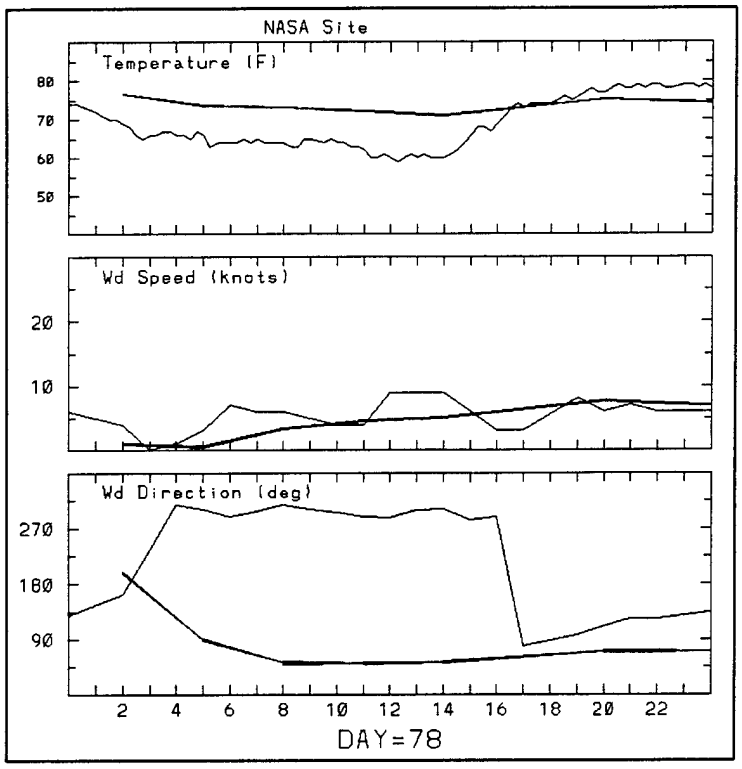

Figure 10C. Same as figure 10A, except for NASA Site (15), by the old BFM at NTC.

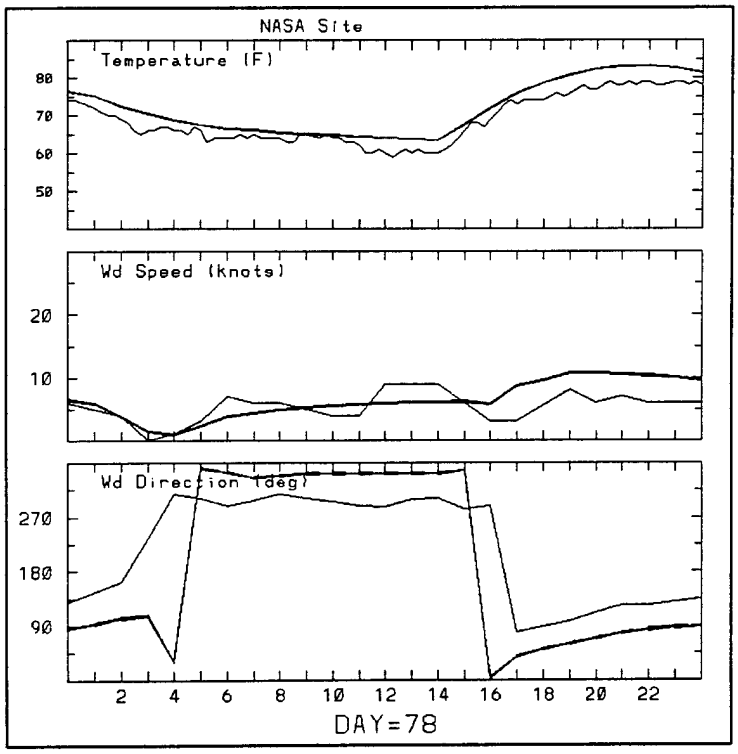

Figure 10D. Same as figure 10A, except for NASA Site (15), by the new BFM.

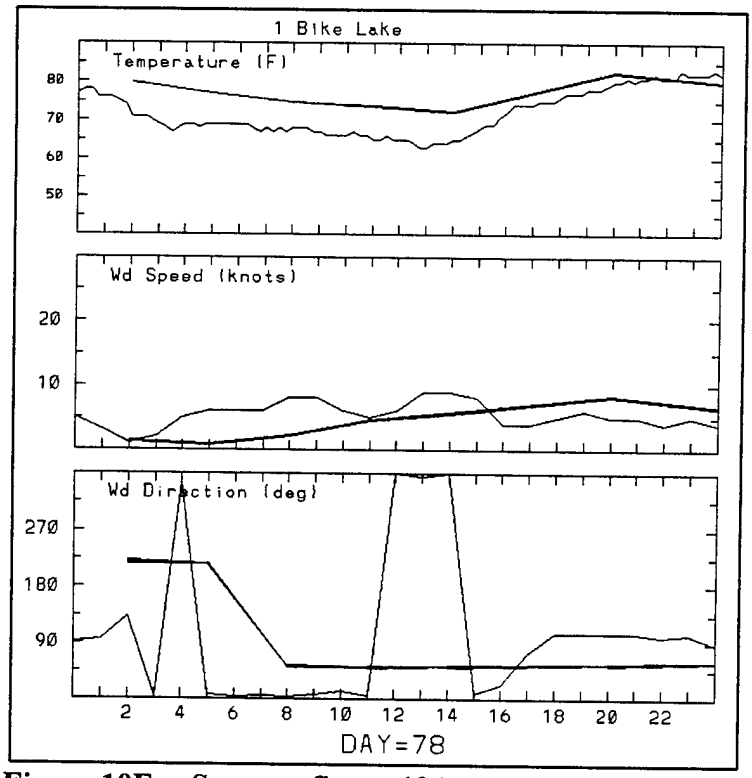

Figure 10E. Same as figure 10A, except for Bike Lake (1), by the old BFM at NTC.

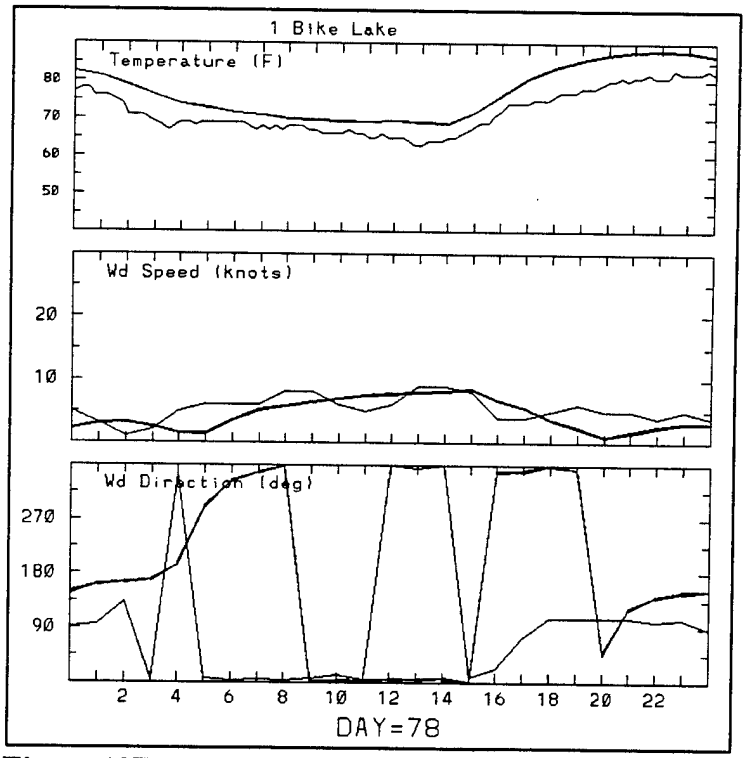

Figure 10F. Same as figure 10A, except for Bike Lake (1), by the new BFM.

If interpolations were made by taking into consideration the effects of altitude differences on temperature, the magnitude of the deviation in figure 10 might have been smaller than the values shown, but interpolation of temperature as a function of altitude would not have corrected the differences seen in figure 10. NOGAPS data used for initialization and time-dependent boundary conditions must also have contributed to the deviation.

- Observed temperature at site 14 (Red Pass Lake) showed consistently lower values than calculation. Comparison of the temperature records throughout TFXXI between site 14 and 1 (Bike Lake), which are located at similar elevations, revealed that the temperatures at site 14 were about 10 to 20 °F consistently lower than those at site 1 (also, see figure 5). Therefore, we conclude that temperature observations at site 14 are inaccurate.

- The magnitudes of wind speed on this day were typically less than 10 kn, and forecast values of wind speed are similar to those observed. The variations of wind direction are better simulated by the new BFM than by the old BFM for all three sites.

Figures 11A through 11D show the surface (10 m above ground) wind vector fields calculated by the old BFM run at NTC. The forecast calculation was initialized at 02Z, 19 March 1997. Figures 11A through 11D represent, respectively, 0, 6, 12, and 18 h forecast fields. In these figures, thick arrows represent observed wind vectors. Agreements between forecast and observation are not as expected. It can seen from figures 11B, 11C, and 11D that calculated wind directions changed slightly throughout the model domain during the 12 h period.

Figures 12A through 12D are the surface wind vector fields at 0 through 18 h calculated by the new BFM. The forecast calculation was initialized at 00Z, 19 March 1997 and extended out to 24 h. The result of the 24 h forecast is not shown. The agreements between calculation and observation are better than those shown in figures 11A through 11D, and the vector fields show substantial diurnal variations due to surface heating and cooling. Notice the variations of wind direction in the northeastern sector of the model domain.

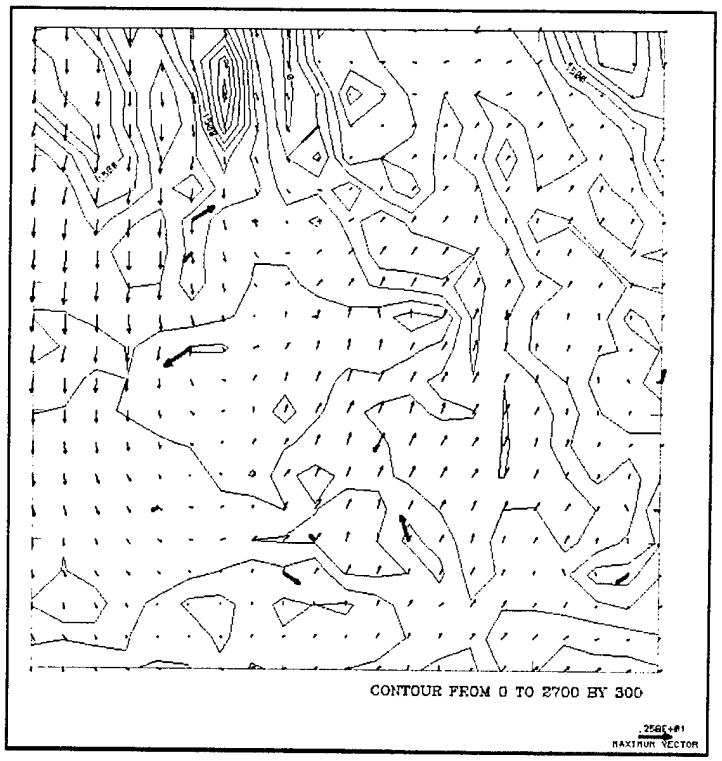

Figure 11A. Surface wind vector field by the old BFM for 19 March, 02 GMT.

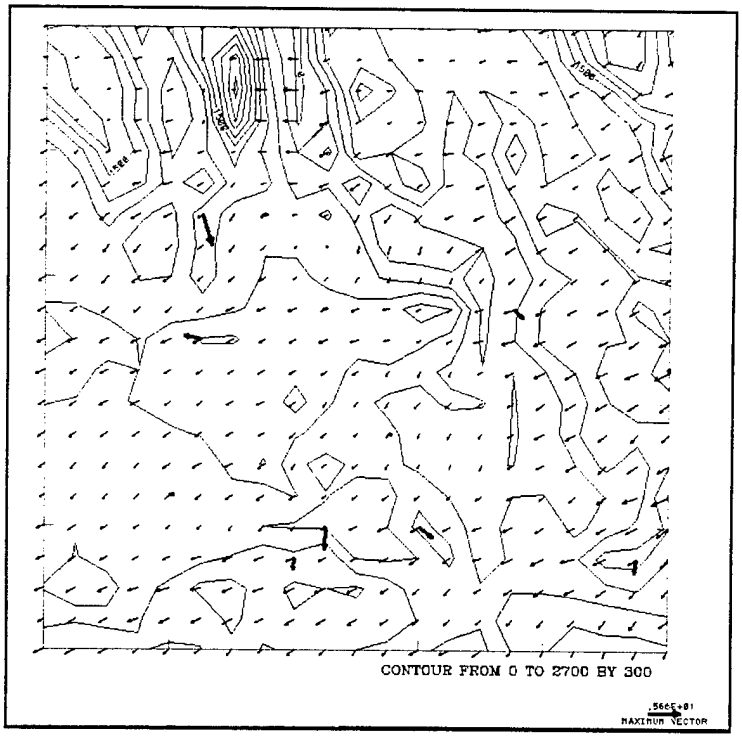

Figure 11B. Same as figure 11A, except for 08 GMT.

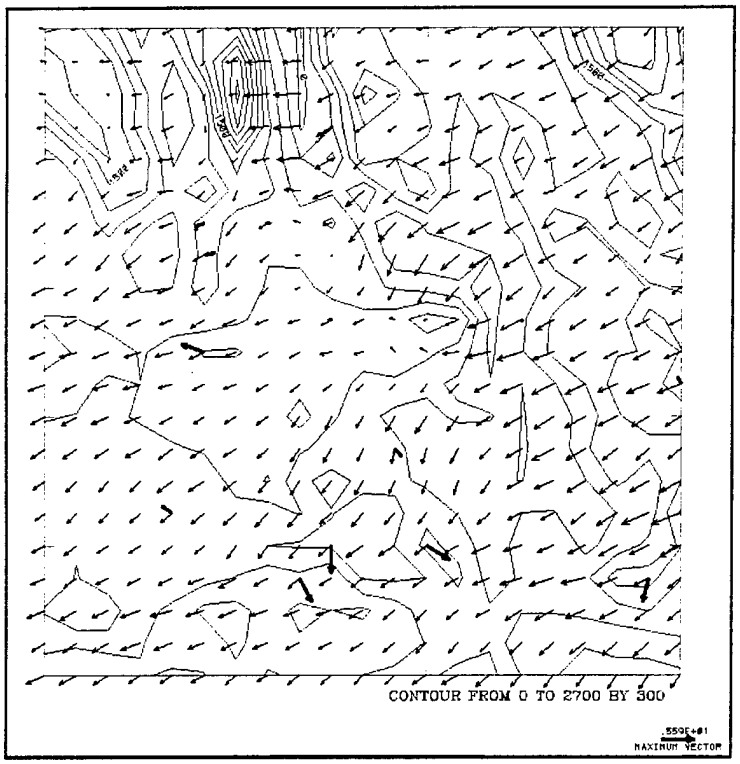

Figure 11C. Same as figure 11A, except for 14 GMT.

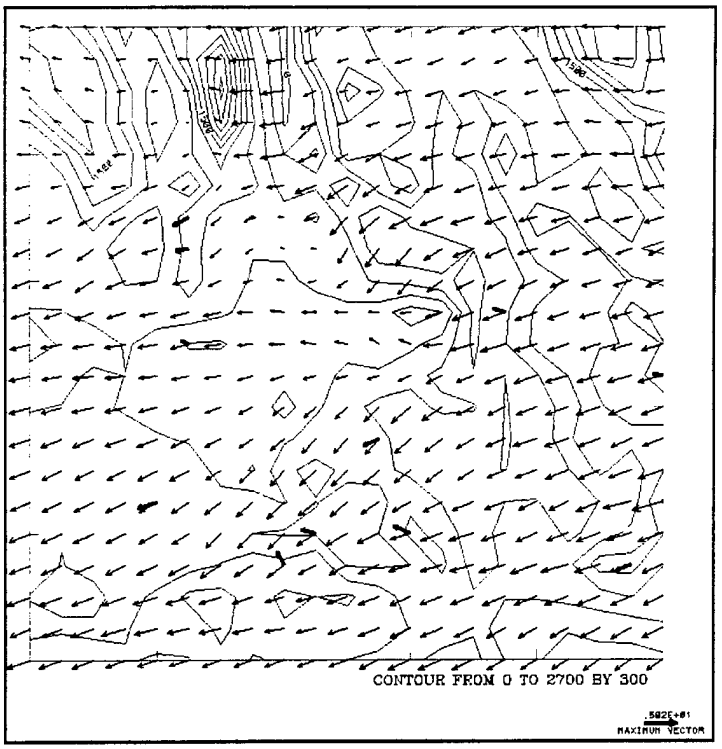

Figure 11D. Same as figure 11A, except for 20 GMT.

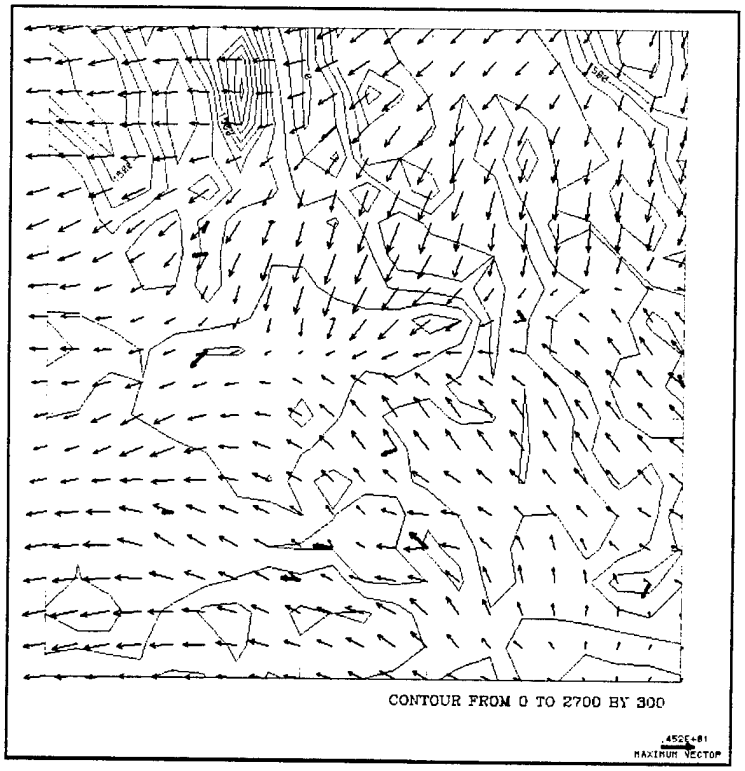

Figure 12A. Surface wind vector field by the new BFM for 19 March, 00 GMT.

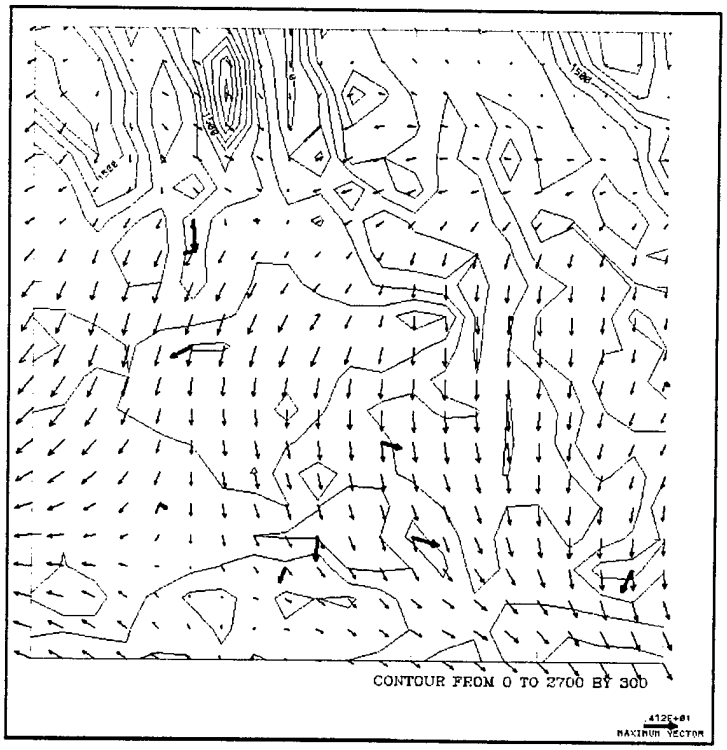

Figure 12B. Same as figure 12A, except for 06 GMT.

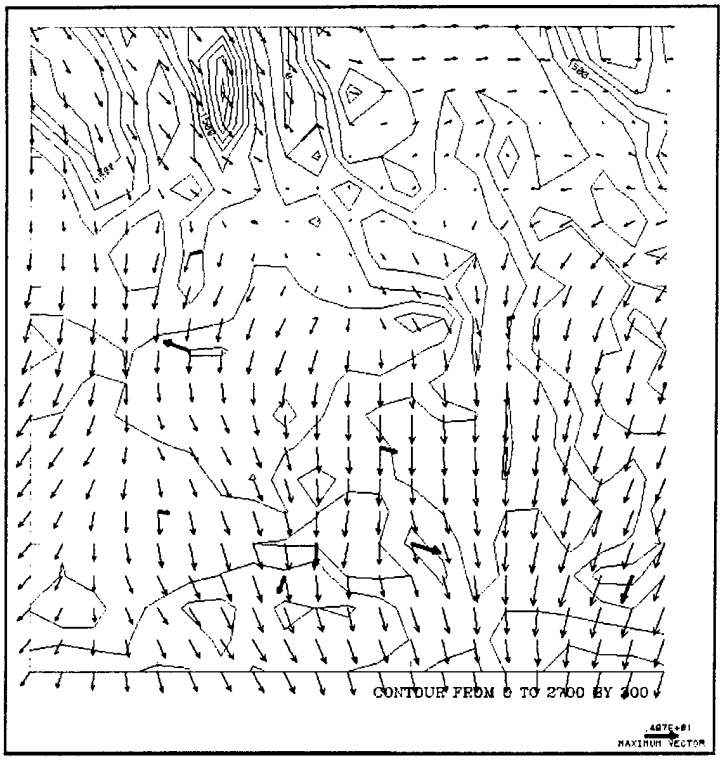

Figure 12C. Same as figure 12A, except for 12 GMT.

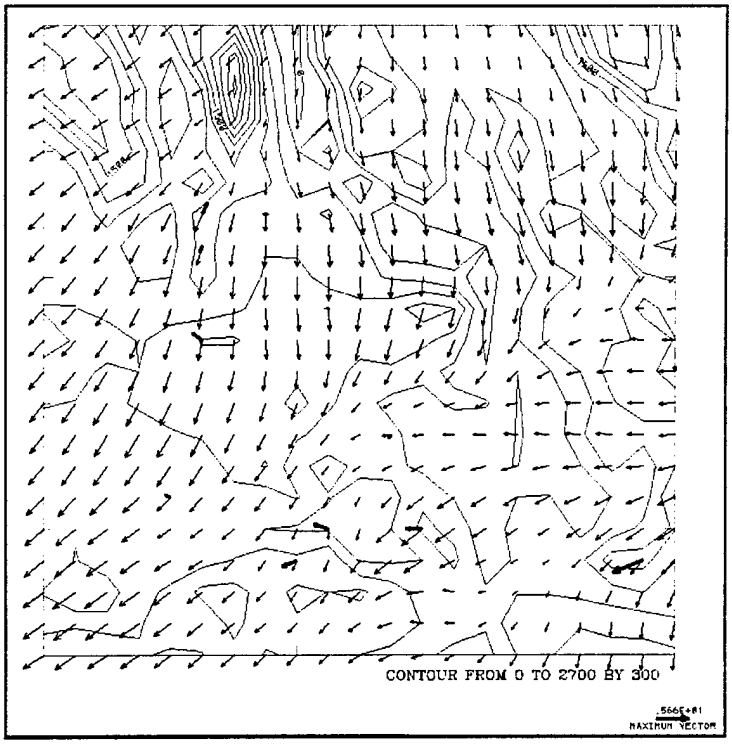

Figure 12D. Same as figure 12A, except for 18 GMT.

Finally, figures 13A through 13D are the scatter diagrams between observation (y-axis) and forecast (x-axis) by the old BFM at NTC, obtained by using all of the data, inclusive of the 0, 6, 9, 12, 18, and 24 h forecast periods, and of nine different cases. Scatter diagrams for temperature, wind speed, x- component of wind (u) and y- component of wind (v) are shown, respectively, in figures 13A through 13D. Corresponding figures, produced from the new BFM, are shown in figures 14A through 14D.

The correlation coefficients between observation and forecast shown in these figures are as follows:

	Old BFM	New BFM
Temperature	0.41	0.61
Wind speed	0.01	0.35
u	0.51	0.47
v	0.33	0.55

As can be seen from the figures and the values of correlation coefficients, the new BFM has produced better correlation between forecast and observation in temperature and wind speed than the old BFM. For the wind component, u, the old BFM produced slightly better results, and for v, the new BFM produced better results.

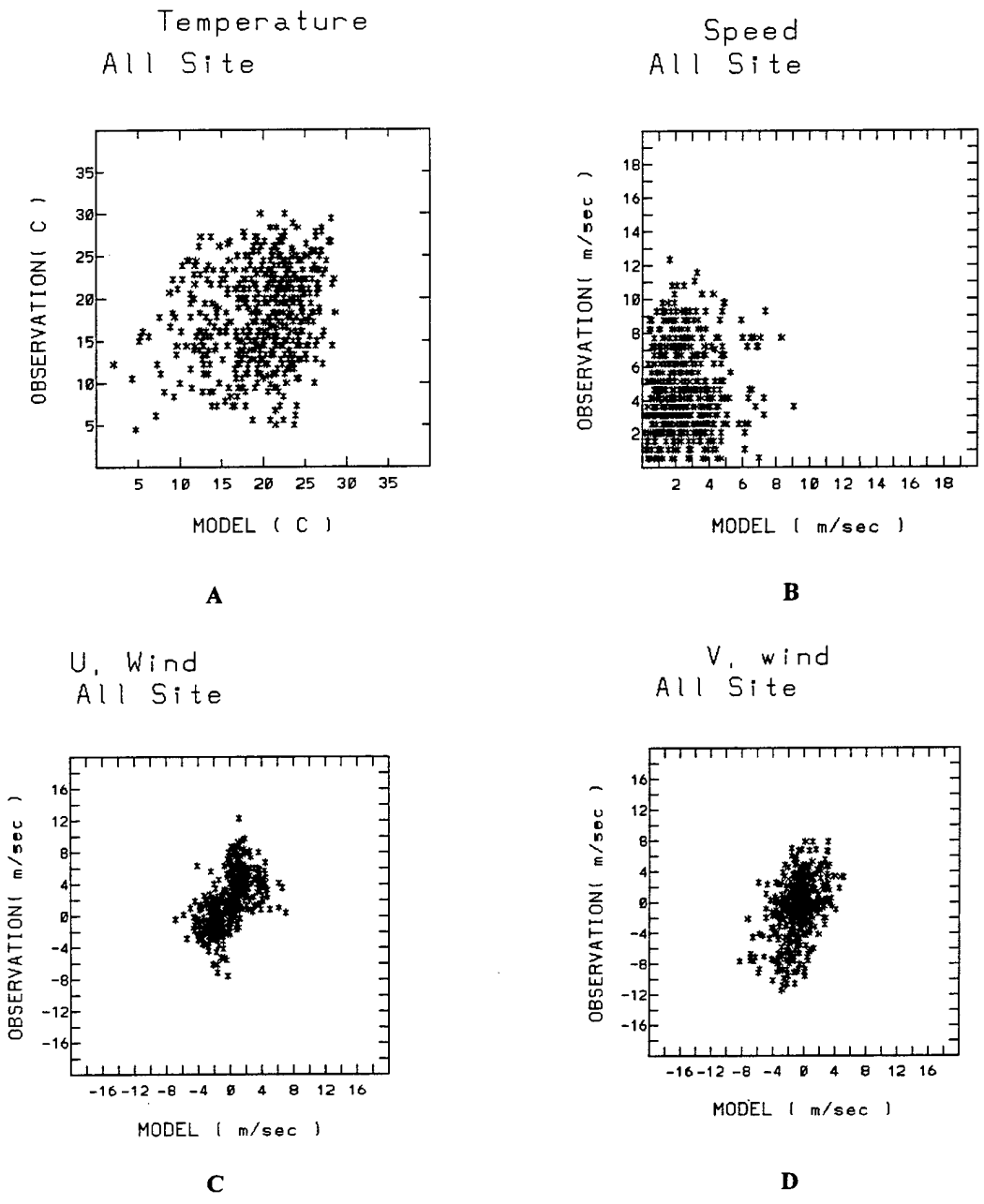

Figure 13. Scatter diagrams of (A) surface temperature, (B) wind speed, (C) x-component of wind, u, and (D) y-component of wind, v, produced by the old BFM.

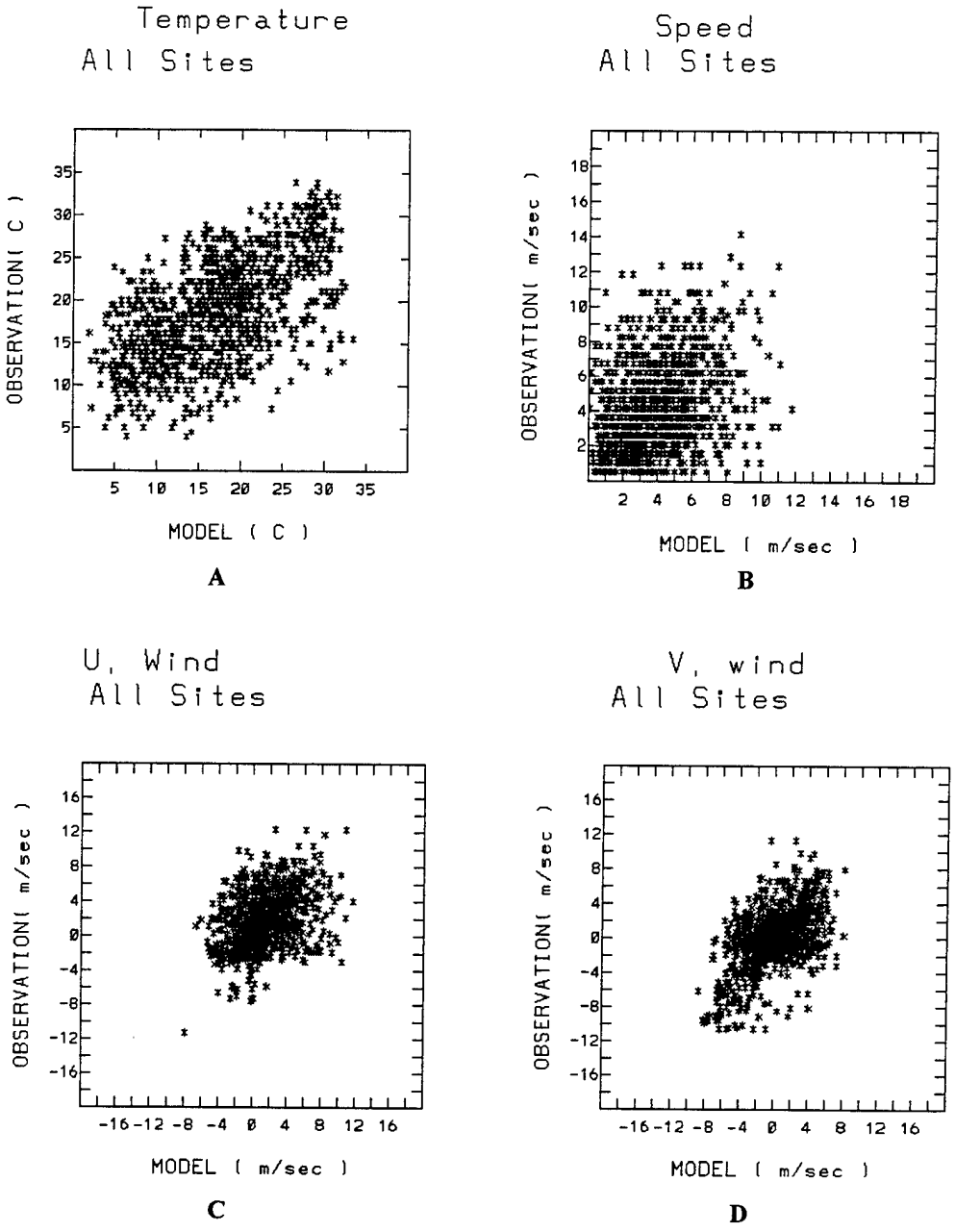

Figure 14. Same as figure 13, except for the new BFM.

5. Summary

The BFM, used operationally for 24 h weather forecasting at NTC during the TFXXI exercise (March 1997), produced several unsatisfactory results. Diurnal variations of surface temperature and wind direction were not as large as the observed variations, and the surface wind speeds during high wind cases were lighter than observation. From the current study, it may be inferred that better forecasting results could have been obtained during the TFXXI exercise by choosing properly the following three items:

- input data for initialization and time-dependent boundary conditions,
- values of ground surface albedo, and of specific heat conductivity of soil, and
- values for nudging coefficients of wind, temperature, and moisture in the boundary layer.

In order to examine the effects of data density, NOGAPS data with 1° grid spacing were used as input data for initialization and for time-dependent boundary conditions. The values of surface albedo and specific conductivity were adjusted for the NTC location (dry and warm desert area). In order to eliminate the damping effects of the nudging terms, which tended to create numerical stagnation effects on meteorological fields in the boundary layer, the nudging terms in the equations of motion, temperature, and mixing ratio were eliminated after the initialization period of 3 h, when the large scale flow was weak.

The following five 24 h forecast datasets, obtained from 16 to 25 March 1997 over the model domain (21 by 21 km, 2.5° grid spacing) covering the NTC, were compared with surface observation data, and statistically analyzed:

(1) archived data of old BFM operated at NTC,
(2) NOGAPS forecast data interpolated spatially and temporally to the BFM model domain,
(3) data from the old BFM obtained by using 1° NOGAPS and surface data for initialization and time-dependent boundary conditions,
(4) data from the new BFM obtained by using 1° NOGAPS data only for both initialization and time-dependent boundary conditions, and
(5) data from the new BFM obtained by using 1° NOGAPS and surface data for initialization and time-dependent boundary conditions.

Dataset (2) produced statistically comparable results to dataset (1), indicating that good input data for initialization and boundary conditions are essential for good forecasting results. It was shown that the old BFM initialized with NOGAPS data (1° grid spacing) produced better forecast fields for both surface temperature and wind speed than the old BFM initialized with NOGAPS (2.5° grid spacing).

The new BFM showed superior performances to the old BFM in surface temperature and wind speed forecasts. The combination of model improvement made in the present study and denser datapoints of NOGAPS with 1° grid spacing are the likely reasons for superior performance. The utilization of surface data for initialization improved the forecasts of surface wind fields for the first several hours of calculation but did little to improve surface temperature fields. There were some questionable observation sites for temperature, so that the above conclusion should be treated as tentative.

The present study also showed that the BFM on a model domain with 2.5 km grid spacing is capable of producing reliable forecast results.

References

1. Henmi, T. and R. Dumais, Jr., *Description of the Battlescale Forecast Model,* TR-1032, U.S. Army Research Laboratory, 1998.

2. Pielke, R. A., *Mesoscale Meteorological Modeling*, Academic Press, Inc., 1984.

3. Panofsky, H. A., A. K. Blackadar, and G. E. McVehil, *The Diabatic Wind Profile*, Quant. J. Roy. Meteorol. Soc., 86, 390-398, 1960.

4. Houghton, D. D., *Handbook of Applied Meteorology*, John Willey & Sons, 1985.

5. Henmi, T., M. E. Lee, and T. J. Smith, "Evaluation of the Battlescale Forecast Model (BFM)," *Proceedings of the 1994 Battlefield Atmospheric Conference,* Battlefield Environment Directorate, U.S. Army Research Laboratory, 1994.

6. Knapp, D. I., and R. E. Dumais, Jr., "Technical Validation of the Battlescale Forecast Model," *Proceedings of the 1995 Battlefield Atmospheric Conference,* Battlefield Environment Directorate, U.S. Army Research Laboratory, 1995.

Acronyms and Abbreviations

AFGWC	U.S. Air Force Global Weather Center
ARL	U.S. Army Research Laboratory
AWDS	Automated Weather Data System
BFM	Battlescale Forecast Model
FNMOC	Fleet Numerical Meteorological and Oceanographical Center
GSM	Global Spectral Model
MEL	Master Environmental Library
NOGAPS	Navy Operational Global Atmospheric Prediction System
NTC	National Training Center
SAMS	surface automated meteorological stations
TFXXI	Task Force XXI

Distribution

	Copies
NASA MARSHAL SPACE FLT CTR ATMOSPHERIC SCIENCES DIV E501 ATTN DR FICHTL HUNTSVILLE AL 35802	1
NASA SPACE FLT CTR ATMOSPHERIC SCIENCES DIV CODE ED 41 1 HUNTSVILLE AL 35812	1
ARMY STRAT DEFNS CMND CSSD SL L ATTN DR LILLY PO BOX 1500 HUNTSVILLE AL 35807-3801	1
ARMY MISSILE CMND AMSMI RD AC AD ATTN DR PETERSON REDSTONE ARSENAL AL 35898-5242	1
ARMY MISSILE CMND AMSMI RD AS SS ATTN MR H F ANDERSON REDSTONE ARSENAL AL 35898-5253	1
ARMY MISSILE CMND AMSMI RD AS SS ATTN MR B WILLIAMS REDSTONE ARSENAL AL 35898-5253	1
ARMY MISSILE CMND AMSMI RD DE SE ATTN MR GORDON LILL JR REDSTONE ARSENAL AL 35898-5245	1
ARMY MISSILE CMND REDSTONE SCI INFO CTR AMSMI RD CS R DOC REDSTONE ARSENAL AL 35898-5241	1
ARMY MISSILE CMND AMSMI REDSTONE ARSENAL AL 35898-5253	1
CMD (420000D(C0245)) ATTN DR A SHLANTA NAVAIRWARCENWPNDIV 1 ADMIN CIR CHINA LAKE CA 93555-6001	1
PACIFIC MISSILE TEST CTR GEOPHYSICS DIV ATTN CODE 3250 POINT MUGU CA 93042-5000	1

NAVAL OCEAN SYST CTR
CODE 54
ATTN DR RICHTER
SAN DIEGO CA 52152-5000 1

METEOROLOGIST IN CHARGE
KWAJALEIN MISSILE RANGE
PO BOX 67
APO SAN FRANCISCO CA 96555 1

DEPT OF COMMERCE CTR
MOUNTAIN ADMINISTRATION
SPRT CTR LIBRARY R 51
325 S BROADWAY
BOULDER CO 80303 1

DR HANS J LIEBE
NTIA ITS S 3
325 S BROADWAY
BOULDER CO 80303 1

NCAR LIBRARY SERIALS
NATL CTR FOR ATMOS RSCH
PO BOX 3000
BOULDER CO 80307-3000 1

DEPT OF COMMERCE CTR
325 S BROADWAY
BOULDER CO 80303 1

DAMI POI
WASHINGTON DC 20310-1067 1

MIL ASST FOR ENV SCI OFC
OF THE UNDERSEC OF DEFNS
FOR RSCH & ENGR R&AT E LS
PENTAGON ROOM 3D129
WASHINGTON DC 20301-3080 1

DEAN RMD
ATTN DR GOMEZ
WASHINGTON DC 20314 1

ARMY INFANTRY
ATSH CD CS OR
ATTN DR E DUTOIT
FT BENNING GA 30905-5090 1

AIR WEATHER SERVICE
TECH LIBRARY FL4414 3
SCOTT AFB IL 62225-5458 1

USAFETAC DNE
ATTN MR GLAUBER
SCOTT AFB IL 62225-5008 1

HQ AFWA/DNX
106 PEACEKEEPER DR STE 2N3
OFFUTT AFB NE 68113-4039 1

PHILLIPS LABORATORY
PL LYP
ATTN MR CHISHOLM
HANSCOM AFB MA 01731-5000 1

ATMOSPHERIC SCI DIV
GEOPHYISCS DIRCTRT
PHILLIPS LABORATORY
HANSCOM AFB MA 01731-5000 1

PHILLIPS LABORATORY
PL LYP 3
HANSCOM AFB MA 01731-5000 1

ARMY MATERIEL SYST
ANALYSIS ACTIVITY
AMXSY
ATTN MR H COHEN
APG MD 21005-5071 1

ARMY MATERIEL SYST
ANALYSIS ACTIVITY
AMXSY AT
ATTN MR CAMPBELL
APG MD 21005-5071 1

ARMY MATERIEL SYST
ANALYSIS ACTIVITY
AMXSY CR
ATTN MR MARCHET
APG MD 21005-5071 1

ARL CHEMICAL BIOLOGY
NUC EFFECTS DIV
AMSRL SL CO
APG MD 21010-5423 1

ARMY MATERIEL SYST
ANALYSIS ACTIVITY
AMSXY
APG MD 21005-5071 1

ARMY MATERIEL SYST
ANALYSIS ACTIVITY
AMXSY CS
ATTN MR BRADLEY
APG MD 21005-5071 1

ARMY RESEARCH LABORATORY
AMSRL D
2800 POWDER MILL ROAD
ADELPHI MD 20783-1145 1

ARMY RESEARCH LABORATORY
AMSRL OP SD TP
TECHNICAL PUBLISHING
2800 POWDER MILL ROAD
ADELPHI MD 20783-1145 1

ARMY RESEARCH LABORATORY
AMSRL OP CI SD TL
2800 POWDER MILL ROAD
ADELPHI MD 20783-1145 1

ARMY RESEARCH LABORATORY
AMSRL SS SH
ATTN DR SZTANKAY
2800 POWDER MILL ROAD
ADELPHI MD 20783-1145 1

ARMY RESEARCH LABORATORY
AMSRL
2800 POWDER MILL ROAD
ADELPHI MD 20783-1145 1

NATIONAL SECURITY AGCY W21
ATTN DR LONGBOTHUM
9800 SAVAGE ROAD
FT GEORGE G MEADE MD 20755-6000 1

ARMY RSRC OFC
ATTN AMXRO GS (DR BACH)
PO BOX 12211
RTP NC 27009 1

DR JERRY DAVIS
NCSU
PO BOX 8208
RALEIGH NC 27650-8208 1

US ARMY CECRL
CECRL GP
ATTN DR DETSCH
HANOVER NH 03755-1290 1

ARMY ARDEC
SMCAR IMI I BLDG 59
DOVER NJ 07806-5000 1

ARMY COMMUNICATIONS
ELECTR CTR FOR EW RSTA
AMSEL EW D
FT MONMOUTH NJ 07703-5303 1

ARMY COMMUNICATIONS
ELECTR CTR FOR EW RSTA
AMSEL EW MD
FT MONMOUTH NJ 07703-5303 1

ARMY DUGWAY PROVING GRD
STEDP MT DA L 3
DUGWAY UT 84022-5000 1

ARMY DUGWAY PROVING GRD
STEDP MT M
ATTN MR BOWERS
DUGWAY UT 84022-5000 1

DEPT OF THE AIR FORCE
OL A 2D WEATHER SQUAD MAC
HOLLOMAN AFB NM 88330-5000 1

PL WE
KIRTLAND AFB NM 87118-6008 1

USAF ROME LAB TECH
CORRIDOR W STE 262 RL SUL
26 ELECTR PKWY BLD 106
GRIFFISS AFB NY 13441-4514 1

AFMC DOW
WRIGHT PATTERSON AFB OH 45433-5000 1

ARMY FIELD ARTILLERY SCHOOL
ATSF TSM TA
FT SILL OK 73503-5600 1

ARMY FOREIGN SCI TECH CTR
CM
220 7TH STREET NE
CHARLOTTESVILLE VA 22448-5000 1

NAVAL SURFACE WEAPONS CTR
CODE G63
DAHLGREN VA 22448-5000 1

ARMY OEC
CSTE EFS
PARK CENTER IV
4501 FORD AVE
ALEXANDRIA VA 22302-1458 1

ARMY CORPS OF ENGRS
ENGR TOPOGRAPHICS LAB
ETL GS LB
FT BELVOIR VA 22060 1

ARMY TOPO ENGR CTR
CETEC ZC 1
FT BELVOIR VA 22060-5546 1

SCI AND TECHNOLOGY
101 RESEARCH DRIVE
HAMPTON VA 23666-1340 1

ARMY NUCLEAR CML AGCY
MONA ZB BLDG 2073
SPRINGFIELD VA 22150-3198 1

USATRADOC
ATCD FA
FT MONROE VA 23651-5170 1

ARMY TRADOC ANALYSIS CTR
ATRC WSS R
WSMR NM 88002-5502 1

ARMY RESEARCH LABORATORY AMSRL IS S INFO SCI & TECH DIR WSMR NM 88002-5501	1
ARMY RESEARCH LABORATORY AMSRL IS E INFO SCI & TECH DIR WSMR NM 88002-5501	1
ARMY RESEARCH LABORATORY AMSRL IS W INFO SCI & TECH DIR WSMR NM 88002-5501	1
DTIC 8725 JOHN J KINGMAN RD STE 0944 FT BELVOIR VA 22060-6218	1
ARMY MISSILE CMND AMSMI REDSTONE ARSENAL AL 35898-5243	1
ARMY DUGWAY PROVING GRD STEDP3 DUGWAY UT 84022-5000	1
USTRADOC ATCD FA FT MONROE VA 23651-5170	1
WSMR TECH LIBRARY BR STEWS IM IT WSMR NM 88001	1
US MILITARY ACADEMY MATHEMATICAL SCI CTR EXCELLENCE DEPT OF MATHEMATICAL SCIENCES ATTN MDN A (MAJ DON ENGEN) THAYER HALL WEST POINT NY 10996-1786	1
ARMY RESEARCH LABORATORY ATTN AMSRL IS EW MR HENMI WSMR NM 88002-5501	10
ARMY RESEARCH LABORATORY ATTN AMSRL IS EW MR DUMAIS WSMR NM 88002-5501	10
Record copy	1
TOTAL	90